

1 **Innovative quantitative PCR assays for the assessment of HIV-associated cryptococcal**
2 **meningoencephalitis in Sub-Saharan Africa**

3
4 Tshepiso Mbangiwa^{1,2,3}, Aude Sturny-Leclère², Kwana Lechiile¹, Cheusisime Kajanga⁴,
5 Timothée Boyer-Chammard^{2,5}, Jennifer C. Hoving^{3,7}, Tshepo Leeme¹, Melanie Moyo⁴, Nabila
6 Youssouf^{1,8}, David S. Lawrence^{1,8}, Henry Mwandumba^{3,9}, Mosepele Mosepele^{1,10}, Thomas S
7 Harrison^{11,12,13}, Joseph N Jarvis^{1,8}, Olivier Lortholary^{2,6,14}, Alexandre Alanio^{2,6,15} on
8 behalf of The Ambition Study Group.
9

10
11 ¹ Botswana-Harvard Health Partnership, Gaborone, Botswana
12 ² Institut Pasteur, Université Paris Cité, CNRS, Unité de Mycologie Moléculaire, UMR2000, F-
13 75015 Paris, France
14 ³ Institute of Infectious Disease and Molecular Medicine, Department of Pathology, Faculty
15 of Health Sciences, University of Cape Town, Cape Town, South Africa
16 ⁴ Malawi-Liverpool-Wellcome Trust Clinical Research Programme, Kamuzu University of
17 Health Science, Blantyre, Malawi
18 ⁵ Department of Infectious Diseases and Tropical Medicine. Centre Hospitalier d'Ajaccio,
19 Ajaccio, France
20 ⁶ Institut Pasteur, Université Paris Cité, Department of Mycology Centre National de
21 Référence Mycoses Invasives et Antifongiques, F-75015 Paris, France
22 ⁷ AFRICA CMM Medical Mycology Research Unit, Institute of Infectious Disease and
23 Molecular Medicine (IDM), Cape Town, South Africa
24 ⁸ Department of Clinical Research, Faculty of Infectious and Tropical Diseases, London
25 School of Hygiene and Tropical Medicine, London, United Kingdom
26 ⁹ Liverpool School of Tropical Medicine, Liverpool, UK
27 ¹⁰ Department of Internal Medicine, University of Botswana, Gaborone, Botswana
28 ¹¹ Centre for Global Health, Institute for Infection and Immunity, St George's University of
29 London, London, United Kingdom
30 ¹² Clinical Academic Group in Infection, St George's University Hospitals NHS Foundation
31 Trust, London, United Kingdom
32 ¹³ MRC Centre for Medical Mycology, University of Exeter, Exeter, United Kingdom
33 ¹⁴ Necker Pasteur Centre for Infectious Diseases and Tropical Médecine, Hôpital Universitaire
34 Necker-Enfants Malades, Assistance Publique Hôpitaux de Paris, Paris, France
35 ¹⁵ Laboratoire de parasitologie-mycologie, AP-HP, Hôpital Saint-Louis, F-75010 Paris, France

NOTE: This preprint reports new research that has not been certified by peer review and should not be used to guide clinical practice.

36 **Abstract**

37 **Background**

38 Cryptococcal meningitis (CM) accounts for about 10-20% of AIDS-defining illnesses with a
39 10-week mortality rate of 25-50%. Fungal load assessed by colony-forming unit (CFU) counts
40 is used as a prognostic marker and to monitor response to treatment in research studies.
41 PCR-based assessment of fungal load could be more rapid and less labor-intensive.

42 **Methods**

43 We developed and validated species-specific qPCR assays based on DNA amplification of a
44 Quorum Sensing Protein 1 (*QSP1*); *QSP1A*, *QSP1 B/C*, and *QSP1 D* that are specific to *C.*
45 *neoformans*, *C. deneoformans* and *C. gattii* species, respectively, and a pan-*Cryptococcus*
46 assay based on a multicopy *28S rRNA* gene. We tested these assays for species identification
47 (*QSP1*) and quantification (*QSP1* and *28S*) on cerebrospinal fluid (CSF) of 209 CM patients at
48 baseline (Day 0) and during anti-fungal therapy (Day 7 and Day 14), from the AMBITION-cm
49 trial in Botswana and Malawi (2018-2021).

50 **Findings**

51 When compared to quantitative cryptococcal culture (QCC) as the reference, the sensitivity
52 of the *28S rRNA* and *QSP1* assays were 98.2% [95% CI: 95.1-99.5] and 90.4% [95% CI: 85.2-
53 94.0] respectively in cerebrospinal fluid (CSF) at Day 0. Quantification of the fungal load
54 with *QSP1* and *28S rRNA* qPCR correlated with QCC ($R^2=0.73$, $R^2=0.78$, respectively). Both
55 Botswana and Malawi had a predominant *C. neoformans* prevalence of 67% [95% CI: 55, 75]
56 and 68% [95% CI: 57, 73], respectively and lower *C. gattii* rates of 21% [95% CI: 14, 31] and
57 8% [95% CI: 4, 14], respectively. We identified 10 patients that, after 14 days of treatment,
58 harboured viable but non-culturable yeasts based on *QSP1* RNA detection (without any
59 positive CFU in CSF culture).

60 **Interpretation**

61 *QSP1* and *28S rRNA* assays are useful in identifying *Cryptococcus* species. qPCR results
62 correlated well with baseline QCC and showed a similar decline in fungal load during
63 induction therapy. These assays have a quick turnaround time and could be used in place of
64 QCC to determine fungal load clearance. The clinical implications of the detection of
65 possibly viable but non-culturable cells in CSF during induction therapy remain unclear.

66

67 **Funding**

68 The AMBITION-cm clinical trial which was funded by the European and Developing Countries
69 Clinical Trials Partnership; Swedish International Development Cooperation Agency;
70 Wellcome Trust / Medical Research Council (UK) / UKAID Joint Global Health Trials and
71 National Institute for Health Research (UK).

72 Background

73 HIV-associated cryptococcal meningitis is the second leading cause of all AIDS-related
74 mortality ¹. An estimated 152,000 cases of cryptococcal meningitis occur each year, leading
75 to approximately 112,000 deaths ². Even with the best available antifungal regimens, ten-
76 week mortality is 25-30% ^{3,4}.

77 *Cryptococcus neoformans* and *Cryptococcus gattii* species complexes are responsible for
78 cryptococcosis in humans, with the former being the predominant causative organism with
79 elevated morbidity and mortality in immunocompromised individuals and the latter
80 predominant in immunocompetent persons, at least in certain areas.⁵ *C. neoformans*
81 species complex can be characterized into serotype A (*C. neoformans*), serotype D (*C.*
82 *deneoformans*) and A-D hybrids, while *C. gattii* species complexes are subdivided into two,
83 serotype B and serotype C including *C. gattii*, *C. bacillisporus*, *C. deuterogattii*, *C. tetragattii*,
84 *C. decagattii* ⁶. qPCR assays have already been developed to discriminate these species on
85 colony DNA ⁷⁻⁹, however, these assays are not suitable for diagnosis, following MIQE
86 guidelines ¹⁰.

87 Methods used to diagnose cryptococcal meningitis include India ink staining, fungal culture
88 and cryptococcal polysaccharide capsular antigen (CrAg) detection. CrAg detection can be
89 performed with lateral flow assays (LFA) which are easy and quick to perform.¹¹⁻¹⁴ However,
90 LFA is primarily qualitative and semi-quantitative but does not correlate with the fungal load
91 under treatment, which could be important for the timely monitoring of patient prognosis.
92 Kinetics of CrAg in patients on treatment cannot be used as a prognostic marker as they do
93 not correlate well with a decline in QCC, CrAg also remains positive even after patients have
94 cleared CFU via QCC, which limits the usefulness of CrAg testing in patient monitoring. ^{14,15}
95 Colony forming units (CFU) counts using quantitative cryptococcal culture (QCC) are
96 performed in research studies to quantify the fungal load of culturable yeasts in the CSF and
97 evaluate early fungicidal activity (EFA)^{16,17}. However, QCC is fastidious and time-consuming.
98 Quantitative PCR (qPCR) allows for DNA quantification and reverse transcriptase PCR (RT-
99 qPCR) allows for whole nucleic acid (WNA) amplification and evaluation of viability by
100 detecting mRNA ¹⁸⁻²¹ and is a potential alternative method to monitor patient response to
101 treatment ²⁰.

102
103 We, therefore, developed and evaluated four qPCR assays to identify *Cryptococcus* species/
104 species complexes and quantify *Cryptococcus* load directly from the CSF. We then validated
105 our assays using CSF samples from participants enrolled in the AMBITION-cm trial to offer
106 an innovative approach to monitor the fungal load dynamics.

107
108

109 **Methods**

110 **Quantitative PCR assays and primer design**

111 Primers specific to *Cryptococcus neoformans* (serotype A), *Cryptococcus deneoformans*
112 (serotype D) and *Cryptococcus gattii* species complex (serotype B or C) were designed using
113 Primer 3 (<http://bioinfo.ut.ee/primer3-0.4.0/>) and checked for secondary structures on
114 OligoAnalyzer Tool (<https://eu.idtdna.com/calc/analyzer>). NCBI primer blast
115 (<https://www.ncbi.nlm.nih.gov/tools/primer-blast/>) was used to check for *in silico*
116 specificity. Two assays were developed, targeting (i) the single copy gene Quorum sensing
117 protein 1 (*QSP1*) and (ii) the multicopy gene *28S rRNA* gene (Figure 1). *QSP1* is a
118 *Cryptococcus* specific gene with no ortholog and paralogs outside *Cryptococcus neoformans*
119 and *gattii* species complexes
120 (https://fungidb.org/fungidb/app/record/gene/CNAG_03012#Taxonomy). The *28S rRNA*
121 gene is known as a repeated gene which is a category of genes that is currently
122 recommended to use to improve the sensitivity of the qPCR assay¹⁰. However, the number
123 of copies can vary from an isolate to another²². Therefore, for precise quantification, a
124 unique gene (here *QSP1*) is preferred, when sensitivity of the detection is not an issue. The
125 *28S rRNA* assay was designed to capture the complete diversity within the *Cryptococcus*
126 *neoformans* and *gattii* species complexes in one single assay as designing a specific assay for
127 each recently described species⁶ is not cost-effective and relevant in routine care.
128 Three *QSP1* assays specific to serotype A (*QSP1A*), D (*QSP1D*) and B/C (*QSP1B/C*) were
129 designed for identification and precise quantification (one copy corresponding to one cell)
130 (Figure 1). The *28S rRNA* assay was designed to be pan-*Cryptococcus* and to improve
131 sensitivity to detect low fungal loads as present in several copy in the genome. A reverse
132 transcriptase qPCR (RT-qPCR) assay detecting *QSP1* mRNA using *QSP1A* primers was used to
133 validate and check *Cryptococcus* viability in the clinical specimens. Indeed, mRNA is one of
134 the most abundant transcript in the *Cryptococcus* cells as depicted in FungiDB
135 (https://fungidb.org/fungidb/app/record/gene/CNAG_03012#TranscriptionSummary). As
136 the mRNA transcript is fragile, more than DNA copies, a decreased detection of mRNA as
137 compared to DNA level was considered as proxy of dead yeasts, with only viable cells
138 allowing the production of an increased quantity of mRNA (Supplemental Figure 2F).

139

140 **Primer specificity**

141 The primers were tested on the *C. neoformans* reference strain H99 cells seeded in
142 phosphate buffered saline (PBS) (simulated CSF) and in healthy blood samples at different
143 concentrations and stored at -80°C for at least 48 hours. This was meant to mimic the
144 storage conditions of the CSF specimens collected during the trial³ before whole nucleic
145 acid extractions were carried out. The assays were tested on all the *C. neoformans* and *C.*
146 *gattii* species complexes, and a panel of 89 other species (Supplementary table 1) and
147 fourteen human DNA samples to rule out cross-reactivity with human DNA and other fungal
148 species.

149

150 **Nucleic acid extractions**

151 For optimization experiments presented in the supplemental material, whole nucleic acids
152 (WNA, representing DNA + RNA) were extracted from PBS seeded with H99 cells using the
153 MagNA Pure 96 Instrument (Roche Diagnostics, Mannheim, Germany) and Viral NA large
154 volume kit (Roche Diagnostics, Mannheim, Germany). Comparison between the DNA blood
155 1000 and pathogen universal 1000 extraction protocols on the extraction machine was done

156 using PBS spiked with H99 cells (simulated CSF). Different pre-treatment conditions known
157 to improve nucleic acid extractions were tested, including untreated (control), bead beating
158 (BB), adding 50µl of proteinase K (PK) and 10 min incubation at 65°C before pre-extraction,
159 and a combination of BB and PK.

160 WNA was extracted from stored patient CSF pellet obtained by centrifugation of 1 mL of CSF
161 and freezing. A Pathogen universal 500 protocol was used for extraction and 100ul of WNA
162 was eluted. The RNA process control Roche kit (Roche Diagnostics, Mannheim, Germany)
163 was used as an internal control in RT-qPCR while a DNA internal control kit (DICR-CY5,
164 Diagenode, Seraing, Belgium) was used in qPCR runs, with a defined virus quantity directly
165 added in the sample before extraction, as recommended.¹⁰

166

167 **Quantitative real-time PCR (qPCR) and RT-qPCR**

168 A Light Cycler® 480-II machine (Roche Diagnostics, Mannheim, Germany) was used for all
169 qPCR and RT-qPCR amplification and quantification cycles (Cq) analysis. A Roche Light Cycler
170 480 probes master kit (Roche Diagnostics, Mannheim, Germany) was used for all qPCR
171 reactions, while a TaqMan™ Fast Virus 1-Step Master Mix kit (Thermo Fisher Scientific Inc,
172 Massachusetts, USA) was used for all RT-qPCR reactions. A 0.5 µM (primer) and 0.2 µM
173 (probe) final concentrations were used for *QSP1*, while 0.4 µM primer and 0.2 µM probe
174 final concentrations were used in the *28S rRNA* assay (Table 1). qPCR reactions were run as
175 following: 95°C 10 min, 50 cycles of 95°C 10 sec and then 58°C 30 sec, and 40°C 30 sec, with
176 an additional initial step at 50°C 5 min for RT-qPCR. All Cq values over 40 were considered
177 negative. All qPCR assays were performed blindly to quantitative cryptococcal culture (QCC)
178 results and all clinical information.

179

180 **Relative expression of QSP1A *in vitro***

181 A total of 10⁶ H99 cells were exposed 65°C for 2 hours (Heat killed) and 1mM of H₂O₂ (H₂O₂
182 killed) 1h with stationary phase as control and extracted using the same procedure as
183 above. QSP1 mRNA expression was compared to actine (*ACT1*) mRNA expression using the
184 method of Pfaffl, considering the efficacy of both assays (QSP1=2; ACT1=1.92)²³

185

186 **Quantification and qPCR efficiency**

187 A 10-fold dilution from the strain H99 cells (*QSP1* A), WM276 cells (*QSP1* B/C) and JEC21
188 cells (*QSP1* D) cells were used to create a standard curve, and extrapolation was used to
189 determine the absolute number of *Cryptococcus* cells present in the sample. Regression
190 lines were constructed by plotting the logarithm of the template concentration versus the
191 corresponding Cq value (Supplemental Figure 1A).

192

193 **Biosynex® CryptoPS antigen screening in plasma**

194 A semi-quantitative lateral flow *Cryptococcus* antigen (CrAg) test (Biosynex, Strasbourg,
195 France) was performed following manufacturer's instructions.^{24,25}

196

197 **Study participants and samples and ethical approvals**

198 We collected samples from 209 participants with CM from Botswana (85/205) and Malawi
199 (124/205) enrolled in the AMBITION-cm randomised controlled trial.³ CSF samples collected
200 at day 0 (D0), day 7 (D7) and day 14 (D14) post-antifungal treatment initiation were tested
201 with QCC, and qPCR and RT-qPCR assays. Plasma samples collected at D0 were screened

202 with a CryptoPS test. QCC and India Ink were performed as already described.²⁶ All ethical
203 approvals were described in previous work.^{26,3}

204

205 **Statistical analysis.** Graph Pad prism 9.4.0 (GraphPad, San Diego, California) was used for
206 statistical analysis and data visualization. Kruskal-Wallis test was used to compare means
207 between three or more matched groups when the data were not normally distributed, while
208 Mann-Whitney tests were used for comparison of 2 groups of data when the data were not
209 normally distributed. P-values <0.05 were considered statistically significant.

210 Results

211

212 Analytical specificity of QSP1 (A, B/C, D) and 28S rRNA assays on *Cryptococcus* spp. strains

213 The 28S rRNA assay was tested on a panel of 93 fungal species DNA, including species
214 closely related to *Cryptococcus*, but also including Ascomycetes species such as *Candida*
215 spp., *Aspergillus* spp., *Saccharomyces* spp., *Fusarium* spp., *Penicillium* spp. (Supplementary
216 Table 1). No cross reaction with non-*Cryptococcus* species complexes strains (100%
217 analytical specificity) was observed. The 28S rRNA assay amplified all *C. neoformans* and *C.*
218 *gattii* species complexes with ratios between of 0.46-1.0 as compared to non-*C.*
219 *neoformans/C. gattii* species complexes harbouring ratios between 0.0126 to 0.3322
220 (Supplementary Figure 1).

221 All QSP1 assays (QSP1 A, QSP1B/C and QSP1 D) were tested on the same 93 fungal species
222 and did not amplify *Filobasidium uniguttulatus*, *Vishniacozyma heimagensis* and
223 *Salicocozyma aerius* (Supplementary Figure 1). QSP1A assay amplified serotype A DNAs
224 with a ratio between 0.6113 and 1.00 except for VNII_T4, VNII_8 and VNBII_Bt1 where the
225 amplification was lower with a ratio between 0.1224 and 0.2745. QSP1A assay was able to
226 perfectly amplify VNIII (AD hybrid) with a ratio of 1, but not *C. deneoformans* and *C. gattii*
227 species (Supplementary Figure 1). QSP1D assay amplified *C. deneoformans* and VNIII (AD
228 hybrid) with a ratio between 0.673 to 1, but not *C. neoformans* and *C. gattii* species.
229 QSP1B/C assay allowed amplification of *C. gattii* species, mainly on *C. gattii* s.s., *C.*
230 *deuteroformans* and *C. tetragattii* (VGI VGIV, VGII) with ratio over 0.7195. However, *C.*
231 *bacillisporus* DNAs were amplified with ratios < 0.1. QSP1B/C assay did not amplify *C.*
232 *neoformans* and *C. deneoformans* DNA.

233

234 Validation of the qPCR assays and extraction procedures

235 We first used spiked samples to optimize and validate our assays. The limit of detection with
236 the QSP1A and the 28S rRNA assay were 50 genomes and 1 genome per reaction,
237 respectively. The efficiency of QSP1A assay was 1.98 (slope=-3.347, $r^2=0.998$), while that of
238 28S rRNA assay was 2.08 (slope=-3.141, $r^2=0.993$, Supplemental Figure 2A). For comparison
239 of pre-extraction procedures, amplification of untreated (control) condition after freezing
240 gave a significantly lower Cq value than the other conditions including bead beating (BB),
241 addition of proteinase K (PK) and BB+PK ($p<0.0001$, $p=0.0297$ and $p<0.0001$, respectively)
242 (Supplementary Figure 2B), suggesting better extraction efficiency. There were no
243 statistically significant differences between the two extraction protocols (Pathogen
244 universal and DNA blood) of CSF tested on the MagNa Pure 96 instrument (Supplementary
245 figure 2C).

246

247 Prevalence of *Cryptococcus* species complexes in Botswana and Malawi

248 We designed species specific QSP1 assays allowing rapid *Cryptococcus* identification in CSF
249 specimens. We first validated QSP1 identification with identification of isolates performed
250 using whole genome sequencing. We obtained an adequate identification in 98.4% of the
251 isolates (Appendix Table 2). Upon screening of clinical CSF samples from baseline (D0) in 209
252 participants, including 85 from Botswana and 124 from Malawi, we found a predominance
253 of *C. neoformans*, 67% [95% CI: 55, 75] in Botswana and 68% [95% CI: 57, 73] in Malawi. The
254 prevalence of *C. gattii* species complex was higher in Botswana (21% [95% CI: 14, 31]) than
255 in Malawi (8% [95% CI: 4, 14]). A total of 8%, and 23% of the samples could not be serotyped
256 in Botswana and Malawi respectively due to low fungal (QSP1 negative, 28S positive). No

257 pure *C. deneoformans* CM was detected in both countries. Of note, three (4%) and one (1%)
258 samples were missing at D0 in Botswana and Malawi, respectively.

259

260 **Cryptococcal species-specific fungal load using *QSP1* and *28S rRNA* assays**

261 We compared the quantification obtained in CSF pellet samples from *neoformans* and *gattii*
262 CM using *QSP1* and *28S rRNA* qPCR assays based on Cq values. There was no statistically
263 significant difference in the initial fungal loads (expressed as quantification cycles, Cq) of *C.*
264 *neoformans* and *C. gattii* CM with *QSP1* assay (35.18 [30.45-38.36] vs. 34.57[31.19-37.32],
265 respectively) or *28S rRNA* assay (28.77 [24.66-32.77] vs. 27.64 [24.87-31.73]) (Figure 2C).
266 This was also observed for QCC, *QSP1* and *28S* assays quantification with absolute yeast
267 number (Figure 3G-I). The difference in Cq value (Δ Cq) between *QSP1* and *28S rRNA* assays
268 for each CSF were significantly different with a Δ Cq of 5.71 [IQR-5.09-6.32], reflecting about
269 50 copies of *28S rRNA* per genome in *C. neoformans* and 6.55 [5.75-7.78], reflecting about
270 100 copies of *28S rRNA* genome in *C. gattii*. This has also been observed in the DNA
271 extracted from strains during prior optimizations (Supplemental Figure 2D).

272

273 **Comparison of quantification using our qPCR assays on different fractions of CSF samples** 274 **and QCC**

275 We quantified DNA using *QSP1* assays and *28S* assays in CSF pellets and in CSF supernatant.
276 We also quantified WNA (RNA+DNA) in the CSF pellet as a potential proxy of the viability of
277 the yeasts present in the pellet. At D0 in CSF pellets, the proportion of positivity with DNA
278 was higher with QCC and *28S rRNA*, with 95% and 94% of positive participants, respectively
279 as compared to *QSP1*, where 88% were positive (Figure 2B). At D14, *QSP1* and *28S rRNA*
280 assays showed an increased proportion of positive samples (43.1% and 68.6%, respectively)
281 as compared to QCC (23.4%).

282 At D0 in CSF pellets, the sensitivity of the *28S rRNA* and *QSP1* assays were 98.2% [IC95 95.1-
283 99.5] and 90.4% [IC95 85.2-94.0] when compared to QCC as the reference standard. Indeed,
284 three QCC-negative CSF were found to be *28S rRNA*- and *QSP1*-positive. The sensitivity was
285 98.0 [IC95 94.4-99.5] and 93.0% [IC95 87.9.1-96.0] when compared to the India ink results.
286 Of note, 27 and 16 India ink-negative CSF samples were found to be positive with *28S rRNA*
287 and *QSP1*, respectively. Specificity could not be calculated as all CSF samples came from
288 participants with CM.

289 Detection of *28S rRNA* DNA in CSF supernatant samples gave a lower proportion of positivity
290 when compared to CSF pellet samples with a maximum difference at D14 (43.2 vs. 68.6%)
291 (Figure 2B). *QSP1* WNA detection positivity was lower as compared to *QSP1* DNA in CSF
292 pellets samples at all timepoints (Figure 2B) but was still more positive at D14 than in
293 samples that were quantified with QCC (34 vs. 23.4% positivity). A Bland-Altman analysis
294 shows an agreement between QCC and *QSP1* or *28S* with a ratio bias of 1.24 \pm 0.28 and 0.90
295 \pm 0.24, respectively (Supplemental Figure 3)

296 We compared the quantification of fungal load with QCC, *QSP1* and *28S rRNA* qPCR assays in
297 CSF pellets samples at D0. We found strong correlations between *QSP1*, *28S rRNA* and the
298 gold standard QCC assay (Figure 2A), with a positive linear relationship between *QSP1* and
299 QCC, $R^2=0.733$ (Figure 2A), *28S rRNA* and QCC, $R^2=0.778$ (Figure 2A), and the R^2 value
300 between the designed assays, *QSP1* vs *28S rRNA* was 0.833 (Figure 2A).

301

302 **Significant decrease of fungal load between D0 and D14 upon treatment initiation with**
303 **QCC, *QSP1* and *28S rRNA* but no cryptococcal fungal load differences between treatment**
304 **arms**

305 *QSP1* and *28S rRNA* assays showed a significant decrease in cryptococcal fungal load
306 between D0 and D7, D7 and D14, and D0 and D14 ($p < 0.0001$) (Figure 3B, 3C), which is
307 similar to the decrease observed with QCC (Figure 3A) . Of note, fungal load dynamics was
308 similar in patients from each arm, thereby suggesting a similar fungicidal activity of the two
309 strategies (Figure 3 D, 3E, 3F).

310

311 **Comparison of CrAg detection in plasma at D0 and quantification of fungal load with QCC,**
312 ***QSP1* and *28S rRNA* in initial CSF**

313 The 151 participants plasma samples which were determined as serotype A or B/C, were
314 tested with CryptoPS at D0, 98 (64.5%) had a positive T1 & T2 band, 49 (32.5%) a positive T1
315 band and 4 (2.6%) were negative. Negative CryptoPS tests were identified in serotype B/C
316 infections (4/24, 16.7%), while all serotype A participants had a positive CryptoPS test in the
317 plasma at D0. This was validated with WGS identification as all negative CryptoPS tests came
318 from *C. tetragattii* cases (Appendix Table 2). In serotype B/C, 4 and 3 samples were negative
319 with CrAg while positive with QCC (Figure 4A) and *QSP1* (Figure 4B) and *28S rRNA* (Figure
320 4C), respectively (data was missing for one sample using *28S rRNA* assay).

321

322 **Quantification of yeasts cells in CSF of participants are mainly from viable and culturable**
323 **cells but can also be viable but non culturable cells (VBNC).**

324 We also wanted to determine if the DNA detected and quantified in CSF came from viable
325 yeasts. We first validated that dead cells *in vitro* had a decreased expression of *QSP1* as
326 compared to the actine gene (*ACT1*) and to stationary phase *Cryptococcus* cell
327 (Supplemental Figure 2F).

328 We used the same *QSP1A* assay but with a reverse transcriptase quantitative PCR (RT-qPCR)
329 allowing the detection and quantification of both *QSP1* mRNA and DNA (WNA
330 amplification). We found that there was an increased quantification of the *QSP1A* using RT-
331 qPCR at all timepoints (D0, D7, D14), $p < 0.0001$, Figure 5 A-C). A gain between 0.8 (D0) and
332 1.1 (D7 and D14) Log Cn cells was observed representing 10-fold more detection of WNA
333 than DNA. This proved that RNA target was present in a higher quantity (around 10 times
334 more) than the *QSP1* DNA gene. During optimizations using the H99 strain, we also found an
335 increased quantification with the RT-qPCR as compared to the qPCR with quantification
336 cycle values of 26.55 [22.86-32.59] and 30.61 [27.46-36.61], $p < 0.0001$, respectively
337 (Supplemental Figure 1E). This suggested that yeasts cells detected in the CSF pellet of the
338 participants were viable, producing more *QSP1* mRNA target than DNA target present in the
339 eluate, showing an active expression of *QSP1* gene in a viable organism.

340 We then compared QCC load and *QSP1* WNA load in individual samples. We noticed that
341 QCC was negative and *QSP1* WNA positive in one sample at D0 and D7 and 17 samples at
342 D14 (Figure 5 D-F, red circles). We thus individualized patients with a negative CSF culture
343 but a positive *QSP1* RT-qPCR assay suggesting that viable but non culturable cryptococci
344 were observed in the CSF during meningitis. The W10 outcome of these patients was 23.5%.

345

346 Discussion

347 Several qPCR and RT-qPCR assays (*QSP1A*, *QSP1B/C* and *QSP1D* and *28S rRNA* assays)
348 allowing *Cryptococcus* load quantification and specific identification of *C. neoformans*, *C.*
349 *deneoformans* and *C. gattii* species complexes were designed, optimized, and clinically
350 evaluated using samples collected during the AMBITION-cm trial.³ The analytical specificity
351 and the sensitivity have been validated and show optimal performance, following dedicated
352 MIQE guidelines.¹⁰ We report optimal qPCR efficiencies of ~100% for all assays. *QSP1* and
353 *28S rRNA* assays were able to detect specified species, as shown in Supplementary figure
354 2A. Based on our results, we therefore recommend using *28S rRNA* assay as a screening
355 assay and when positive to identify the species and quantify the fungal load with *QSP1*
356 species specific assays.

357 Interestingly, we identified a high burden of *C. gattii* species complex infections in
358 Botswana (21%) as compared to Malawi (8%) as already reported in those countries (being,
359 13% and 30% for Malawi and Botswana, respectively).^{27,28} No *C. deneoformans* (serotype D)
360 cases was detected in the cohort, as already shown in patients native from Africa and
361 leaving in Europe.²⁹

362 The designed *QSP1* and *28S rRNA* assays showed excellent correlation with QCC
363 quantification. QCC is the current gold standard in cryptococcal fungal load quantification
364 with a reported 94.2% sensitivity in South Africa and Uganda.¹³ We clearly observed a gap
365 between QCC and DNA detection with an increased number of participants detected with
366 the *QSP1* and *28S rRNA* qPCR assays than QCC, suggesting that yeasts unable to grow on
367 culture media or dead yeasts can be detected by qPCR especially at low fungal loads.
368 Nevertheless, participants had lower fungal loads at D7 and/or D14, than the initial load at
369 D0, demonstrating the early fungicidal activity of the two different treatment arms. This
370 finding is important as a decrease of the fungal load and a fungicidal activity could be
371 determined using qPCR quantification instead of QCC.¹⁷ We are currently working at
372 validating our assay in patients with CM and receiving both antiretroviral and antifungal
373 therapies to discriminate relapse from immune reconstitution inflammatory syndrome.

374 By using whole nucleic acids amplification with our *QSP1* assay, which allows amplification
375 of *QSP1* mRNA and DNA, we validated here that most of the yeasts detected, even at D14,
376 were viable, with an increased WNA detection compared to DNA detected. We thus
377 detected DNA (qPCR) in participants with negative QCC results at D0 D7 and D14 and
378 significantly more amplification with *QSP1* WNA (RT-qPCR), suggesting that living yeasts
379 were present in the CSF despite a negative culture at D0, D7 or D14. These cells are
380 suggestive of viable but non culturable cells (VBNC), meaning viable living yeasts but not
381 capable of growth on agar plates. This phenotype is known in *Cryptococcus* yeasts cells and
382 have been identified and characterized recently by our team.^{30,31} This is a major finding as
383 RT-qPCR should be better at characterizing the presence of viable cells as compared to QCC.
384 It tends to show that VBNC can be found in CSF and that antifungal treatment could induce
385 this phenomenon. More work needs to be done to investigate those VBNC in human CSF
386 under treatment.

387 In a study done by Tenforde et al. in Botswana assessing the sensitivity and specificity of
388 CryptoPS, the sensitivity was found to be 61.0% and the specificity to be 96.6%.²⁴
389 Additionally, it has been shown recently that the CryptoPS test was not detecting in vitro
390 capsular antigens from *C. gattii* species complex including *C. bacillisporus*, *C. deuterogattii*
391 and *C. tetragattii* species.³² Our results show that there are false negative results only in
392 serotype B/C infections but not with serotype A. The high prevalence of serotype B/C (*C.*

393 *gattii* species complex) infections in Botswana (see above) might explain the low sensitivity
394 rate that was previously reported when using CryptoPS locally.
395 In conclusion, we designed and validated three qPCR in three assays (*QSP1 A*, *QSP1 B/C*, and
396 *28S rRNA*) for the detection and quantification of *Cryptococcus* spp. (*28S*) in CSF. These
397 assays have excellent correlation with the current gold standard, i.e QCC. qPCR will thus
398 provide easier fungal load monitoring tool and early information on subsequent outcome
399 during HIV-associated cryptococcal meningitis in sub-Saharan Africa. As a diagnostic tool
400 that can speciate and give fungal load, it enables stratified management of patients in the
401 future. Our assays can be used as research tools to measure clearance more quickly and
402 easily as an endpoint to assess novel antifungal regimens.
403
404

405 **Acknowledgments**

406 We thank Vincent Enouf and Tiffany Dos Santos from the P2M facility, Institut Pasteur for
407 their help on the MagNa Pure instrument. We warmly want to thank Philippa Griffin-
408 Johnstone, the administrative manager during the Ambition trial her extensive and precious
409 administrative support. We would also like to thank the AMBITION-cm team, especially
410 personnel in Blantyre and Gaborone, together with Dr Sumayah Salie, Dr Charlotte Schutz
411 and Dr Muki Shey in UCT for their assistance with paperwork in UCT. We thank the
412 AMBITION-cm trial participants and their families and caregivers, as well as all the clinical,
413 laboratory, and administrative staff at all the sites who were not directly involved in the
414 trial; Andrew Nunn, Sayoki Mfinanga, Robert Peck, and William Powderly for serving on the
415 data and safety monitoring committee; and John Perfect, Andrew Kambugu, Saidi Kapigi,
416 and Douglas Wilson for serving on the trial steering committee.

417

418 **Funding**

419 Funded by a grant through the European Developing Countries Clinical Trials Partnership
420 (EDCTP) supported by the Swedish International Development Cooperation Agency (SIDA)
421 (TRIA2015-1092), and the U.K. Department of Health and Social Care, the U.K. Foreign
422 Commonwealth and Development Office, the U.K. Medical Research Council, and Wellcome
423 Trust, through the Joint Global Health Trials scheme (MR/P006922/1). Trial registration
424 number: ISRCTN72509687. This work was also funded by the National Institute for Health
425 Research (NIHR) through a Global Health Research Professorship to JNJ (RP-2017-08-ST2-
426 012) using UK aid from the UK Government to support global health research. The funders
427 did not influence the design, execution, and analysis of data from the study. This
428 (publication) was made possible (in part) by a grant from Carnegie Corporation of New York.
429 The statements made and views expressed are solely the responsibility of the author.

430

431 References

- 432 1. Rajasingham R, Smith RM, Park BJ, et al. Global burden of disease of HIV-associated
433 cryptococcal meningitis: an updated analysis. *Lancet Infect Dis* 2017; **17**(8): 873-81.
- 434 2. Rajasingham R, Govender NP, Jordan A, et al. The global burden of HIV-associated
435 cryptococcal infection in adults in 2020: a modelling analysis. *Lancet Infect Dis* 2022.
- 436 3. Jarvis JN, Lawrence DS, Meya DB, et al. Single-Dose Liposomal Amphotericin B Treatment for
437 Cryptococcal Meningitis. *N Engl J Med* 2022; **386**(12): 1109-20.
- 438 4. Molloy SF, Kanyama C, Heyderman RS, et al. Antifungal Combinations for Treatment of
439 Cryptococcal Meningitis in Africa. *N Engl J Med* 2018; **378**(11): 1004-17.
- 440 5. Mohamed SH, Nyazika TK, Ssebambulidde K, Lionakis MS, Meya DB, Drummond RA. Fungal
441 CNS Infections in Africa: The Neuroimmunology of Cryptococcal Meningitis. *Front Immunol* 2022; **13**:
442 804674.
- 443 6. Hagen F, Khayhan K, Theelen B, et al. Recognition of seven species in the *Cryptococcus*
444 *gattii*/*Cryptococcus neoformans* species complex. *Fungal Genet Biol* 2015; **78**: 16-48.
- 445 7. Satoh K, Maeda M, Umeda Y, Miyajima Y, Makimura K. Detection and identification of
446 probable endemic fungal pathogen, *Cryptococcus gattii*, and worldwide pathogen, *Cryptococcus*
447 *neoformans*, by real-time PCR. *Microbiol Immunol* 2011; **55**(6): 454-7.
- 448 8. Aoki FH, Imai T, Tanaka R, et al. New PCR primer pairs specific for *Cryptococcus neoformans*
449 serotype A or B prepared on the basis of random amplified polymorphic DNA fingerprint pattern
450 analyses. *J Clin Microbiol* 1999; **37**(2): 315-20.
- 451 9. Leal AL, Faganello J, Bassanesi MC, Vainstein MH. *Cryptococcus* species identification by
452 multiplex PCR. *Med Mycol* 2008; **46**(4): 377-83.
- 453 10. Bustin SA, Benes V, Garson JA, et al. The MIQE guidelines: minimum information for
454 publication of quantitative real-time PCR experiments. *Clin Chem* 2009; **55**(4): 611-22.
- 455 11. Williamson PR, Jarvis JN, Panackal AA, et al. Cryptococcal meningitis: epidemiology,
456 immunology, diagnosis and therapy. *Nat Rev Neurol* 2017; **13**(1): 13-24.
- 457 12. Rajasingham R, Wake RM, Beyene T, et al. Cryptococcal Meningitis Diagnostics and
458 Screening in the Era of Point-of-Care Laboratory Testing. *Journal of Clinical Microbiology* 2019; **57**(1):
459 e01238-18.
- 460 13. Boulware DR, Rolfes MA, Rajasingham R, et al. Multisite validation of cryptococcal antigen
461 lateral flow assay and quantification by laser thermal contrast. *Emerg Infect Dis* 2014; **20**(1): 45-53.
- 462 14. Temfack E, Rim JJB, Spijker R, et al. Cryptococcal Antigen in Serum and Cerebrospinal Fluid
463 for Detecting Cryptococcal Meningitis in Adults Living With Human Immunodeficiency Virus:
464 Systematic Review and Meta-Analysis of Diagnostic Test Accuracy Studies. *Clin Infect Dis* 2021; **72**(7):
465 1268-78.
- 466 15. Perfect JR, Bicanic T. Cryptococcosis Diagnosis and Treatment: What Do We Know Now.
467 *Fungal genetics and biology : FG & B* 2015; **78**: 49-54.
- 468 16. Bicanic T, Brouwer AE, Meintjes G, et al. Relationship of cerebrospinal fluid pressure, fungal
469 burden and outcome in patients with cryptococcal meningitis undergoing serial lumbar punctures.
470 *Aids* 2009; **23**(6): 701-6.
- 471 17. Loyse A, Wilson D, Meintjes G, et al. Comparison of the early fungicidal activity of high-dose
472 fluconazole, voriconazole, and flucytosine as second-line drugs given in combination with
473 amphotericin B for the treatment of HIV-associated cryptococcal meningitis. *Clin Infect Dis* 2012;
474 **54**(1): 121-8.
- 475 18. Latouch S, Totet A, Lacube P, Bolognini J, Nevez G, Roux P. Development of an RT-PCR on the
476 heat shock protein 70 gene for viability detection of *Pneumocystis carinii* f. sp. *hominis* in patients
477 with pneumocystosis and in air sample. *J Eukaryot Microbiol* 2001; **Suppl**: 176s-7s.
- 478 19. Demirci M, Saribas S, Ozer N, et al. Diagnostic performance of the RT-qPCR method targeting
479 85B mRNA in the diagnosis of pulmonary *Mycobacterium tuberculosis* infection. *J Infect Public*
480 *Health* 2018; **11**(5): 662-6.

- 481 20. Alanio A, Gits-Muselli M, Lanternier F, et al. Evaluation of a New Histoplasma spp.
482 Quantitative RT-PCR Assay. *J Mol Diagn* 2021; **23**(6): 698-709.
- 483 21. Dellière S, Hamane S, Aissaoui N, Gits-Muselli M, Bretagne S, Alanio A. Increased sensitivity
484 of a new commercial reverse transcriptase-quantitative PCR for the detection of Pneumocystis
485 jirovecii in respiratory specimens. *Med Mycol* 2021; **59**(8): 845-8.
- 486 22. Alanio A, Sturny-Leclère A, Benabou M, Guigue N, Bretagne S. Variation in copy number of
487 the 28S rDNA of Aspergillus fumigatus measured by droplet digital PCR and analog quantitative real-
488 time PCR. *J Microbiol Methods* 2016; **127**: 160-3.
- 489 23. Pfaffl MW. A new mathematical model for relative quantification in real-time RT-PCR.
490 *Nucleic Acids Res* 2001; **29**(9): e45.
- 491 24. Tenforde MW, Boyer-Chammard T, Muthoga C, et al. Diagnostic Accuracy of the Biosynex
492 CryptoPS Cryptococcal Antigen Semiquantitative Lateral Flow Assay in Patients with Advanced HIV
493 Disease. *J Clin Microbiol* 2020; **59**(1).
- 494 25. Aissaoui N, Benhadid-Brahmi Y, Sturny-Leclère A, et al. Investigation of CryptoPS LFA-
495 positive sera in patients at risk of cryptococcosis. *Med Mycol* 2022; **60**(10).
- 496 26. Lawrence DS, Youssouf N, Molloy SF, et al. AMBIsome Therapy Induction Optimisation
497 (AMBITION): High Dose AmBisome for Cryptococcal Meningitis Induction Therapy in sub-Saharan
498 Africa: Study Protocol for a Phase 3 Randomised Controlled Non-Inferiority Trial. *Trials* 2018; **19**(1):
499 649-.
- 500 27. Chen Y, Litvintseva AP, Frazzitta AE, et al. Comparative analyses of clinical and
501 environmental populations of Cryptococcus neoformans in Botswana. *Mol Ecol* 2015; **24**(14): 3559-
502 71.
- 503 28. Steele KT, Thakur R, Nthobatsang R, Steenhoff AP, Bisson GP. In-hospital mortality of HIV-
504 infected cryptococcal meningitis patients with *C. gattii* and *C. neoformans* infection in Gaborone,
505 Botswana. *Med Mycol* 2010; **48**(8): 1112-5.
- 506 29. Cogliati M. Global Molecular Epidemiology of Cryptococcus neoformans and Cryptococcus
507 gattii: An Atlas of the Molecular Types. *Scientifica (Cairo)* 2013; **2013**: 675213.
- 508 30. Hommel B, Sturny-Leclère A, Volant S, et al. Cryptococcus neoformans resists to drastic
509 conditions by switching to viable but non-culturable cell phenotype. *PLoS Pathog* 2019; **15**(7):
510 e1007945.
- 511 31. Alanio A, Vernel-Pauillac F, Sturny-Leclère A, Dromer F. Cryptococcus neoformans host
512 adaptation: toward biological evidence of dormancy. *mBio* 2015; **6**(2).
- 513 32. Shi D, Haas PJ, Boekhout T, Hahn RC, Hagen F. Neglecting Genetic Diversity Hinders Timely
514 Diagnosis of Cryptococcus Infections. *J Clin Microbiol* 2021; **59**(4).

515

516 **The AMBITION study group:**

517

518 In addition to the named authors, the following were members of the Ambition Study
519 Group:

520 Botswana Harvard AIDS Institute Partnership / Princess Marina Hospital, Gaborone,
521 Botswana – J Goodall, N Mawoko, J Milburn, R Mmipi, C Muthoga, P Ponatshego, I
522 Rulaganyang, K Seatla, N Tlhako and K Tsholo.

523 University of Cape Town / Mitchells Plain Hospital / Khayelitsha District Hospital, Cape
524 Town, South Africa – S April, A Bekiswa, L Boloko, H Bookholane, T Crede, L Davids, R
525 Goliath, S Hlungulu, R Hoffman, H Kyepa, N Masina, D Maughan, T Mnguni, S Moosa, T
526 Morar, M Mpalali, J Naude, I Oliphant, S Sayed, L Sebesho, M Shey and L Swanepoel.

527 Malawi-Liverpool-Wellcome Trust Clinical Research Programme / Queen Elizabeth Central
528 Hospital, Blantyre, Malawi – M Chasweka, W Chimang'anga, T Chimphambano, E Dziwani, E

529 Gondwe, A Kadzilibile, S Kateta, E Kossam, C Kukacha, B Lipenga, J Ndaferankhande, M
530 Ndalama, R Shah, A Singini, K Stott and A Zambasa.
531 UNC Project, Kamuzu Central Hospital, Lilongwe, Malawi – T Banda, T Chikaonda, G Chitulo,
532 L Chiwoko, N Chome, M Gwin, T Kachitosi, B Kamanga, M Kazembe, E Kumwenda, M
533 Kumwenda, C Maya, W Mhango, C Mphande, L Msumba, T Munthali, D Ngoma, S Nicholas, L
534 Simwinga, A Stambuli, G Tegha and J Zambezi.
535 Infectious Diseases Institute / Kiruddu General Hospital, Kampala, Uganda – C Ahimbisibwe,
536 A Akampurira, A Alice, F Cresswell, J Gakuru, D Kiiza, J Kisémbó, R Kwizera, F Kugonza, E
537 Laker, T Luggya, A Lule, A Musubire, R Muyise, O Namujju, J Ndyetukira, L Nsangi, M
538 Okirwoth, A Sadiq, K Tadeo, A Tukundane and D Williams.
539 Infectious Diseases Institute / Mbarara Regional Referral Hospital, Mbarara, Uganda – L
540 Atwine, P Buzaare, M Collins, N Emily, C Inyakuwa, S Kariisa, J Mwesigye, S Niwamanya, A
541 Rodgers, J Rukundo, I Rwomushana, M Ssemusu and G Stead.
542 University of Zimbabwe / Parirenyatwa General Hospital, Harare, Zimbabwe – K Boyd, S
543 Gondo, P Kufa, E Makaha, C Moyo, T Mtisi, S Mudzingwa, T Mwarumba and T Zinyandu.
544 Institut Pasteur, Paris, France - Françoise Dromer
545 London School of Hygiene and Tropical Medicine, London, UK – P Griffin and S Hafeez.

546 **Figure Legend:**

547 **Figure 1:** Schematic representation of the different assays used in this study

548 *Cryptococcus neoformans* (Cn); whole nucleic acids (WNA), CSF (Cerebrospinal fluid),
549 quantitative real time PCR (qPCR), reverse transcriptase quantitative PCR (RT-qPCR).

550

551 **Figure 2:** Positive correlations between *QSP1* quantification (Log₁₀ Cn cells/mL, *QSP1* Log₁₀
552 Cn) and QCC (Log₁₀ Cn cells/mL, QCC Log₁₀ Cn), *28S rRNA* quantification (Log₁₀ Cn cells/mL,
553 *28S* Log₁₀ Cn) and QCC and *28S rRNA* and *QSP1* using CSF pellet results at day 0 (D0, before
554 starting antifungal treatment) (A). Percentage of CSF pellet and supernatant samples
555 amplified by *QSP1* A, B/C and *28S rRNA* at Day 0 (D0) , Day 7 (D7) and Day 14 (D14) of
556 antifungal treatment (B). Fungal loads in CSF at D0 with *QSP1* and *28S rRNA* assays
557 expressed as quantification cycles in *C. neoformans* and *C. gattii* (C). ****, p<0.0001; ns, not
558 significant.

559 **Figure 3:** Cryptococcal fungal load quantification (Log₁₀ Cn cells/mL, Log₁₀ Cn) at Day 0 (D0),
560 Day 7 (D7) and Day 14 (D14) in CSF of participants by QCC, *QSP1* assay, and *28S rRNA* assay
561 in total populations (A,B,C respectively) and in the control or single dose regimens (D, E, F
562 respectively). Serotype specific fungal load quantification at Day 0 by QCC, *QSP1* and *28S*
563 *rRNA* (G,H,I). **, p<0.001 ****, p<0.0001; ns, not significant.

564 **Figure 4:** Quantification of the fungal load in CSF (Log₁₀ Cn cells/mL, Log₁₀ Cn) of
565 participants with T1-T2 positive band, T1 band and negative CryptoP/S testing in plasma at
566 Day 0 (D0) in serotype A or B/C infections with QCC (A), *QSP1* (B) and *28S* (C) qPCR. ***,
567 p<0.001; ****, p<0.0001

568 **Figure 5:** *QSP1* DNA (qPCR) and WNA (RTqPCR) quantification in CSF pellet at Day 0 (D0) (A),
569 Day 7 (D7) (B) and Day 14 (D14) (C) using *QSP1* assays (A-C), and comparison between QCC
570 and *QSP1* WNA load at Day 0 (D0), Day 7 (D7) (E) and Day 14 (D14) (F). ****, p<0.0001. Red
571 circles are participants with negative QCC and positive *QSP1* WNA detection

572

573 **Supplementary figure 1: Analytical specificity of the different assays.** A heat map showing
574 amplification of *C. neoformans*, *C. gattii* species and other *Cryptococcus* species
575 (*F.uniguttulatus*, *V. haemaeyensis*, *S. aerius*) by *28S rRNA*, *QSP1A*, *QSP1D* and *QSP1B/C*
576 assays based on the ratio of Cq value tested / Cq value of the reference DNA.

577 *Serotype A (VNI, VNII, VNBI, VNBII), serotype D (VNIV), serotype B/C (VGI, VGII, VGIIIa, VGIIIb, VGIIIc, VGIV).
578 Serotype AD (VNIII). Ratios 0-0.3 indicate no amplification to poor amplification, 0.4-0.6 low amplification, and
579 0.7-1.0 good to very good amplification.

580 **Supplementary Figure 2: Implementation and technical validation of the different qPCR**
581 **assays.** Efficiency of *QSP1* A and *28S rRNA* (A), untreated condition yielded more DNA than
582 treatment with bead beating (P<0.001) and proteinase K (p=0.0297)(B). There were no
583 differences in nucleic acid extractions between pathogen universal and DNA blood protocol
584 (C). *QSP1A* and *28S rRNA* Cq from simulated CSF samples seeded with different
585 concentrations of H99 (D) and comparison of Cq between *QSP1A* DNA and *QSP1A* WNA
586 using H99 cells (E). ns, not significant; *, p<0.05; ****, p<0.0001. Relative expression of
587 *QSP1* mRNA to actine (ACT1) mRNA in heat killed or H₂O₂ killed H99 Cn cells as compared to
588 stationary phase H99 (F).

589 **Supplementary Figure 3: Blant-Altman analysis of** Bland-Altman analysis comparing cell
590 quantification between QCC and *QSP1A* (A) or *28S* (B) by plotting the ratio of each pair of
591 value against the average of them. The lines represent the bias (solid line) and the 95%
592 agreements (dotted lines).

593

594 **Table 1:** Species specific primer and probe sets that were designed and used in this study.

595

Primer/Probe	Sequence (5'-3')	Melting temperature (°C)	Length (bp)	Amplicon length (pb)
H99_QSP1_RNA_F2	ACCACTCTTTTCACTGCTG	56,2	19	105
H99_QSP1_RNA_R2	GGCGCCGAAGTTGTTAG	56,6	17	
H99_QSP1_RNA_P2	CTTGTCTCATCGCCCCGGCCCTC	71,9	24	
WM276_QSP1_F2	ACCACACTTTTCACTGCCG	56,2	19	105
WM276_QSP1_R2	GGCACCGAAGTTCTGAG	56,6	17	
WM276_QSP1_P3	CTTGTCTCATCGCCCCTGCCCTC	65.5	24	
JEC21_QSP1_F2	ACCACCCTTTTCACTGCTG	56,2	19	105
JEC21_QSP1_R2	GGCGCCGAAGTTCTGAG	56,6	17	
JEC21_QSP1_P2	CTTGTCTCATCGCCCCGGCCCTC	71,9	24	
AMB_28S_rRNA_F3	GCAGGTCTCCAAGGTGAA	52,8	18	137
AMB_28S_rRNA_R4	CCAGCTTCCTTCCGTCAA	55,0	18	
AMB_28S_rRNA_P4	TTGGCTCTAAGGGTTGGGTGCGTCGGG	67.7	27	

596

597 H99, *C. neoformans*; WM276, *C. gattii*; JEC21; *C. deneoformans*; F, Forward primer; R,
598 Reverse primer; P, Probe.

599

600

601

602

603

604

605 **Supplementary table 1: Fungal species DNA used to test the analytical specificity of the**
606 **primers.**

Number #	Strain ID	Species	Number #	Strain ID	Species
#01	8.1143	Saksenaea vasiformis	#45	16.134	Saccharomyces cerevisia
#02	9.1166	Cunninghamella bertholletiae	#46	15.353	Malassezia pachydermatis
#03	7.1036	Apophysomyces elegans	#47	15.762	Malassezia furfur
#04	14.375	Mucor indicus	#48	MDO	Malassezia sympodialis
#05	12.6	Rhizopus arrhizus var arrhizus	#49	16.024	Cryptococcus neo. var. grubii
#06	8.137	Rhizopus arrhizus var delemar	#50	16.213	Cryptococcus neo. var. neoformans
#07	14.351	Rhizopus microsporus	#51	16.245	Cryptococcus neoformans hybrid AD
#08	14.832	Rhizomucor pusillus	#52	16.289	Cryptococcus gattii sero B
#09	CBS 100.49	Lichtheimia ramosa	#53	CBS 24.79	Trichosporon Asahii
#10	CBS 213.78-2	Syncephalastrum racemosum	#54	CBS 24.66	Trichosporon Cutaneum
#11	CBS 158.50	Coekeroomyces recurvatus	#55	16.076	Phoma saxea
#12	14.128	Conidiobolus coronatus	#56	16.153	Pyrenochaeta unguis-hominis
#13	13.188	Rhizomucor miehei	#57	16.285	Chaetomium globosum
#14	16.241	Mucor circinelloides	#58	14.126	Curvularia inequalis
#15	15.466	Aspergillus nidulans	#59	15.349	Curvularia pseudolonata
#16	15.710	Aspergillus flavus	#60	15.352	Alternaria alternata species group
#17	ATCC 204305	Aspergillus fumigatus	#61	15.365	Alternaria infectoria species group
#18	15.743	Aspergillus niger	#62	16.008	Cladophialophora bantiana
#19	15.439	Aspergillus terreus	#63	16.033	Roussoella percutanea
#20	14.633	Aspergillus versicolor	#64	16.075	Scedosporium apiospermum
#21	14.184	Aspergillus calidoustus	#65	16.161	Coccidioides spp.
#22	15.515	Penicillium rubens	#66	16.186	Emmonsia pasteuriana
#23	15.506	Penicillium lanosocoeruleum	#67	16.205	Histoplasma capsulatum
#24	11.287	Penicillium chrysogenum species complex	#68	15.461	Medicopsis romeroi
#25	11.811	Penicillium citreonigrum (a priori)	#69	15.016	Phaeoacremonium parasiticum
#26	12.077	Penicillium piceum	#70	12.968	Madurella mycetomatis
#27	12.816	Penicillium sg serie Islandica	#71	15.632	Lomentospora prolificans
#28	15.095	Penicillium roquefortii	#72	16.281	Thermothelomyces thermophila
#29	15.517	Fusarium solani sp complex	#73	15.408	Fonsecaea pedrosoi
#30	14.829	Fusarium oxysporum sp complex	#74	15.589	Fonsecaea nubica
#31	14.295	Fusarium fujikuroi sp complex	#75	15.832	Fonsecaea monophora
#32	15.561	Fusarium dimerum sp complex	#76	10.286	Sporothrix sp.
#33	15.483	Fusarium incarnatum equiseti	#77	14.144	Exophiala dermatitis
#34	14.34	Sarocladium kiliense	#78	15.862	Aspergillus quadrilineatus
#35	CBS 430.66	Acremonium curvulum	#79	13.565	Aspergillus sublatus
#36	16.291	Candida albicans	#80	15.313	Neosartorya hiratsukae
#37	16.324	Candida glabrata	#81	13.647	Aspergillus tamarii
#38	16.260	Candida parapsilosis	#82	15.659	Aspergillus parasiticus species comple
#39	16.301	Candida tropicalis	#83	13.583	Aspergillus alabamensis
#40	16.329	Candida krusei	#84	16.146	Bisifusarium delphinoides
#41	16.179	Candida kefyr	#85	6.937	Acremonium sclerotigenum-A egyptia
#42	16.280	Candida lusitaniae	#86	16.22	Scopulariopsis brevicaulis
#43	16.198	Candida dubliniensis	#87	12.216	Scopulariopsis flava
#44	16.216	Candida guilliermondii	#88	15.863	Microascus gracilis
			#89	13.18	Beauveria bassiana
			#90	15.609	Trichoderma orientale
			#91	16.113	Trichoderma longibrachiatum
			#92	16.267	Purpureocillium lilacinum
			#93	13.020	Aureobasidium pullulans

607
608
609
610
611
612
613
614

615 **Supplementary table 2** : Correlation between whole genome sequencing identification of
 616 the recovered isolate and *QSP1A* identification and CrAg testing (Biosynex test) in CSF and
 617 plasma

	qPCR assay			Biosynex in CSF	
	<i>QSP1A</i>	<i>QSP1B/C</i>	<i>QSP1D</i>	Negative	Positive
<i>Cryptococcus</i> species upon WGS of isolate	n (%)	n (%)	n (%)	n (%)	n (%)
<i>Cryptococcus neoformans</i>	104/104 (100)	ND	ND	0/101 (0)	101/101 (100)
<i>C. neoformans C. deneoformans</i> hybrids	4/4 (100)	ND	ND	0/4 (0)	4/4 (100)
<i>Cryptococcus tetragattii</i>	2/16 (12.5)	14/16 (87.5)	ND	3/13 (23)	10/13 (77)
<i>Cryptococcus gattii</i>	0 (0)	4/4 (100)	ND	0/4 (0)	4/4 (100)

618 ND, not done

619

multicopy DNA target



Sensitive Cn cell detection
=> 28S rRNA qPCR

CSF
pellet



Increased detection of Cn DNA
Pan-Cryptococcus

unicopy DNA target

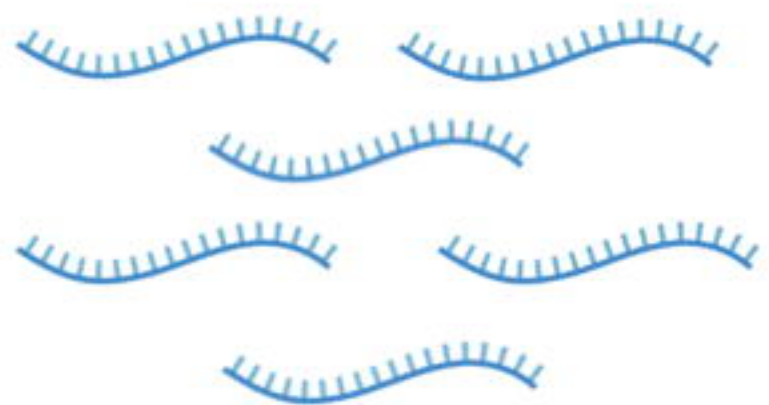


Cn cell quantification assay
+ Identification assay
=> QSP1 qPCR



One DNA copy per cell
Species complex specific assays

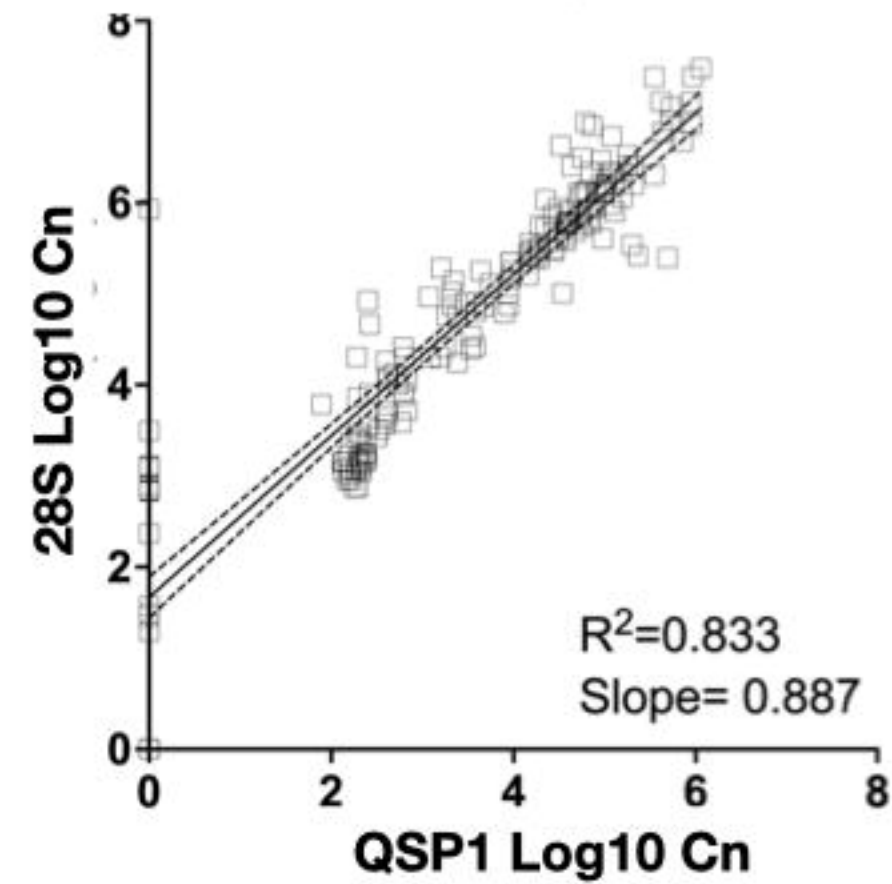
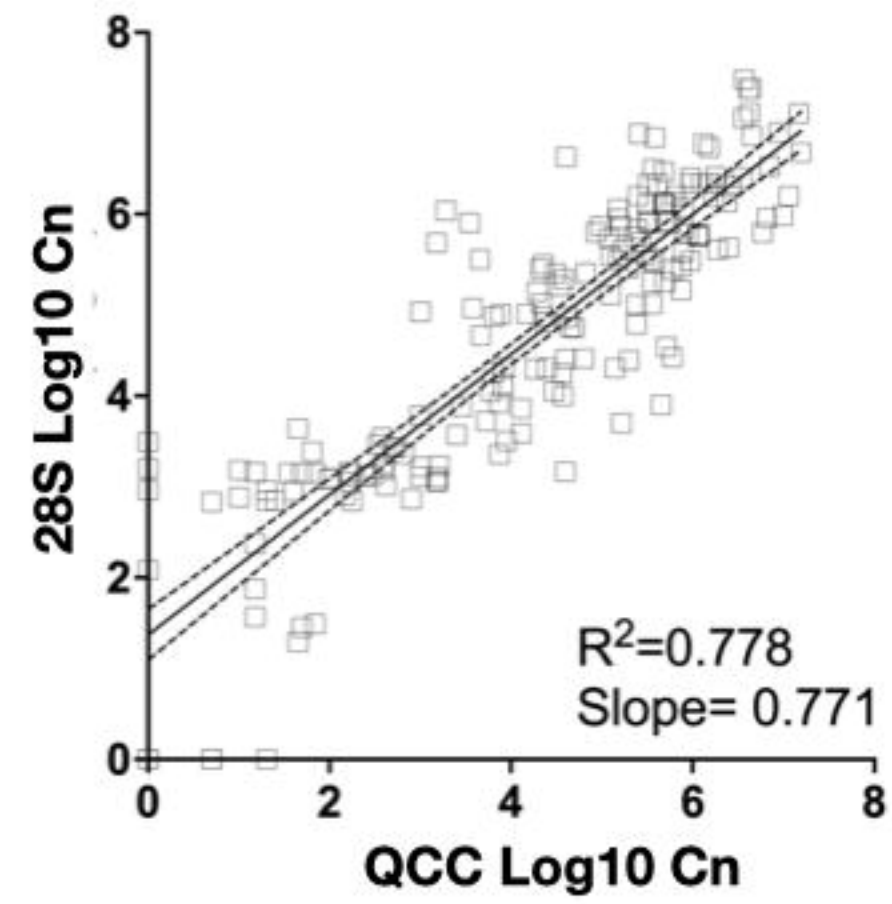
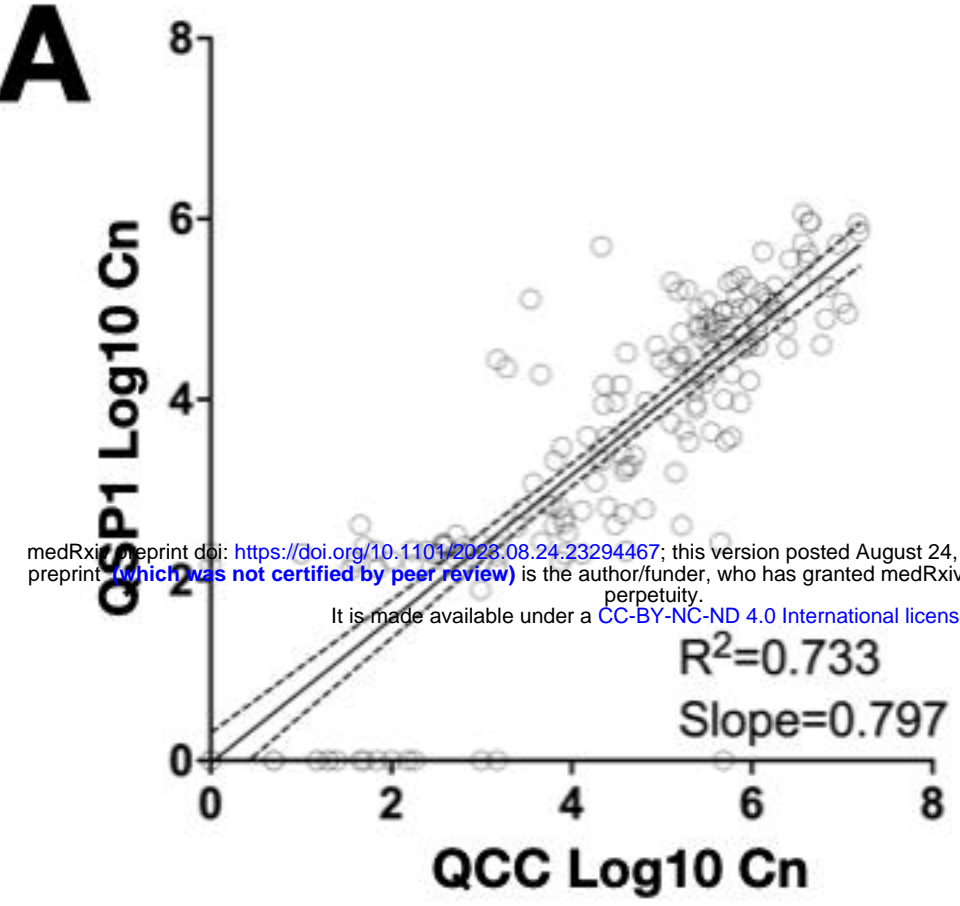
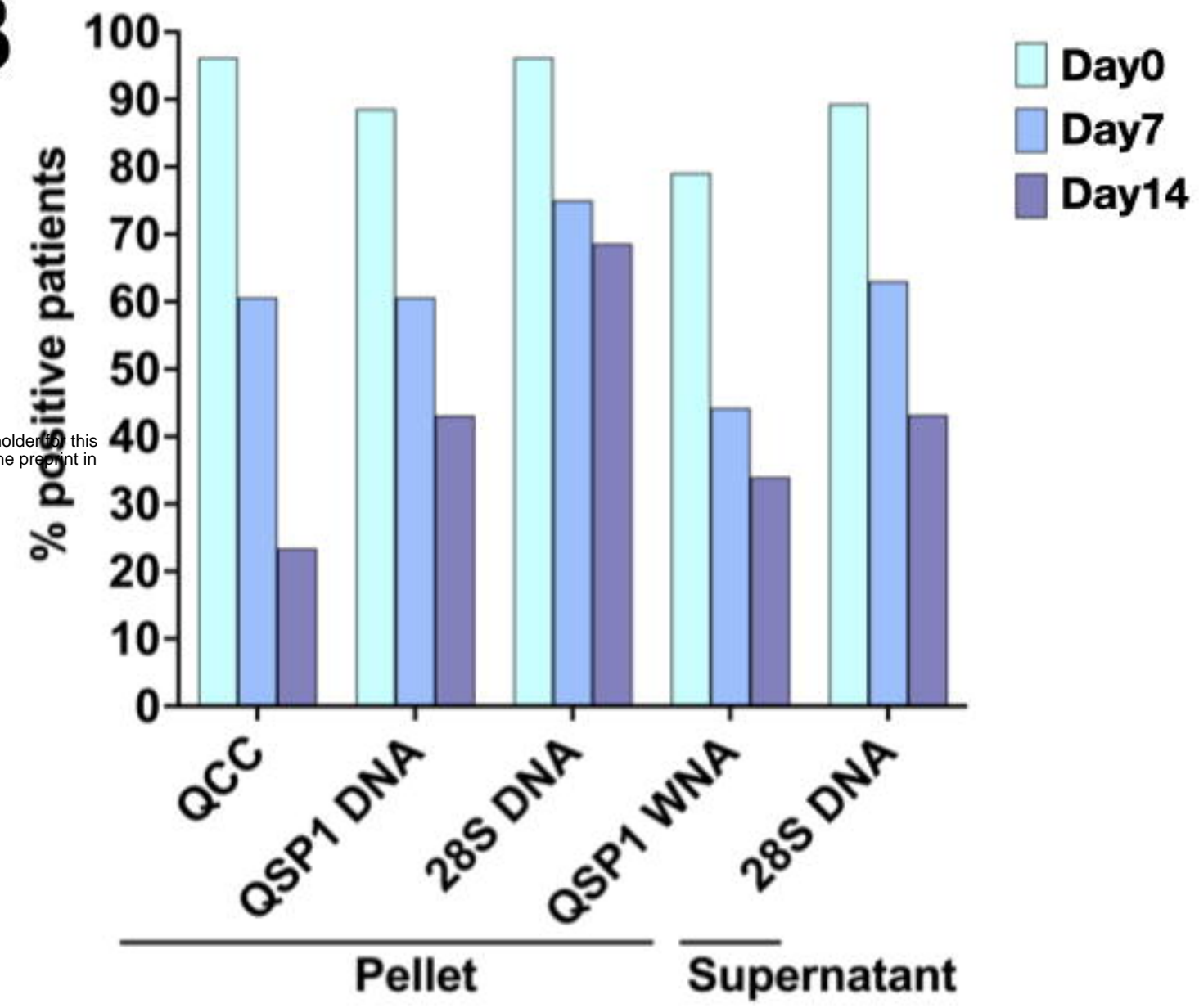
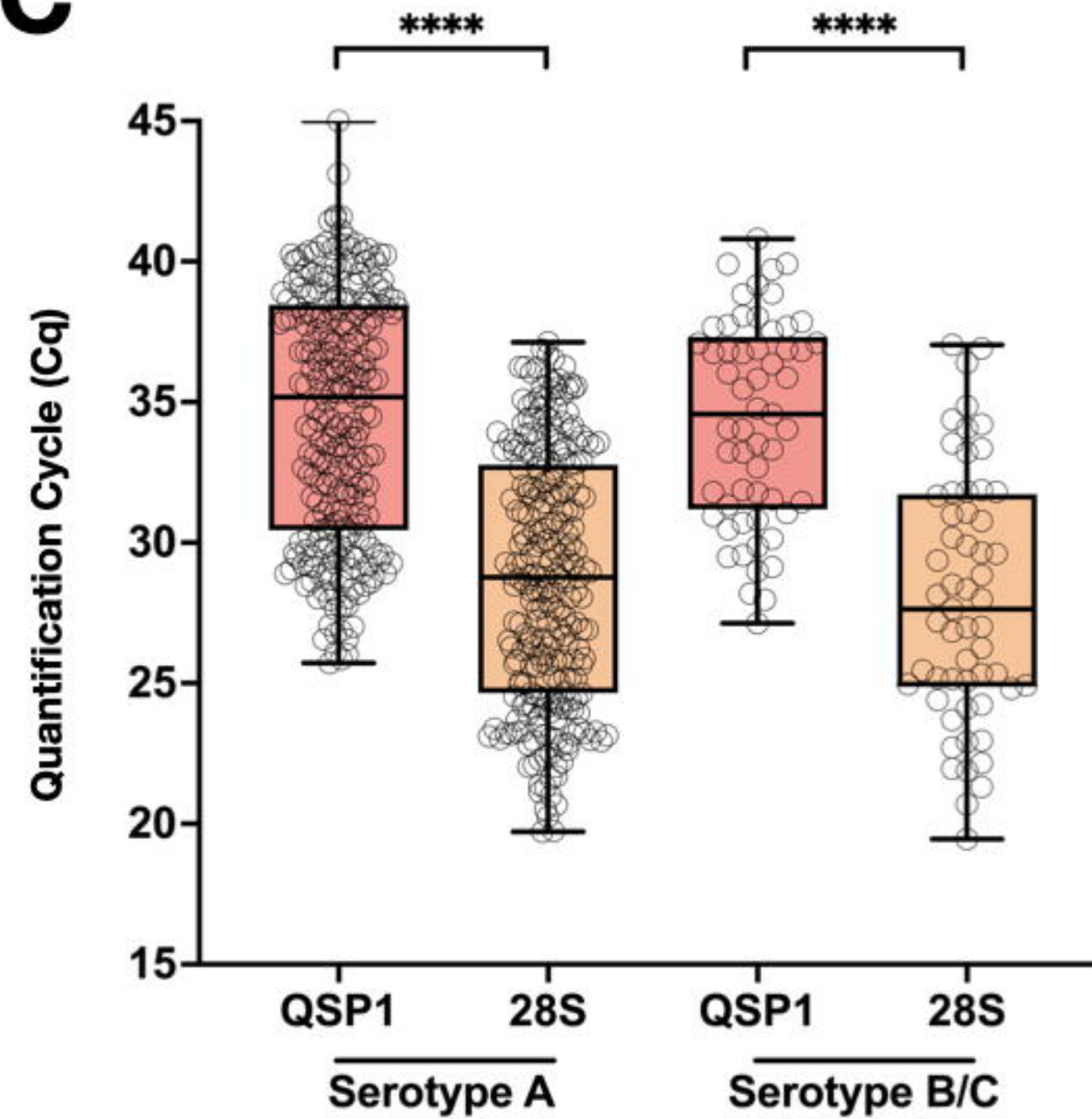
mRNA

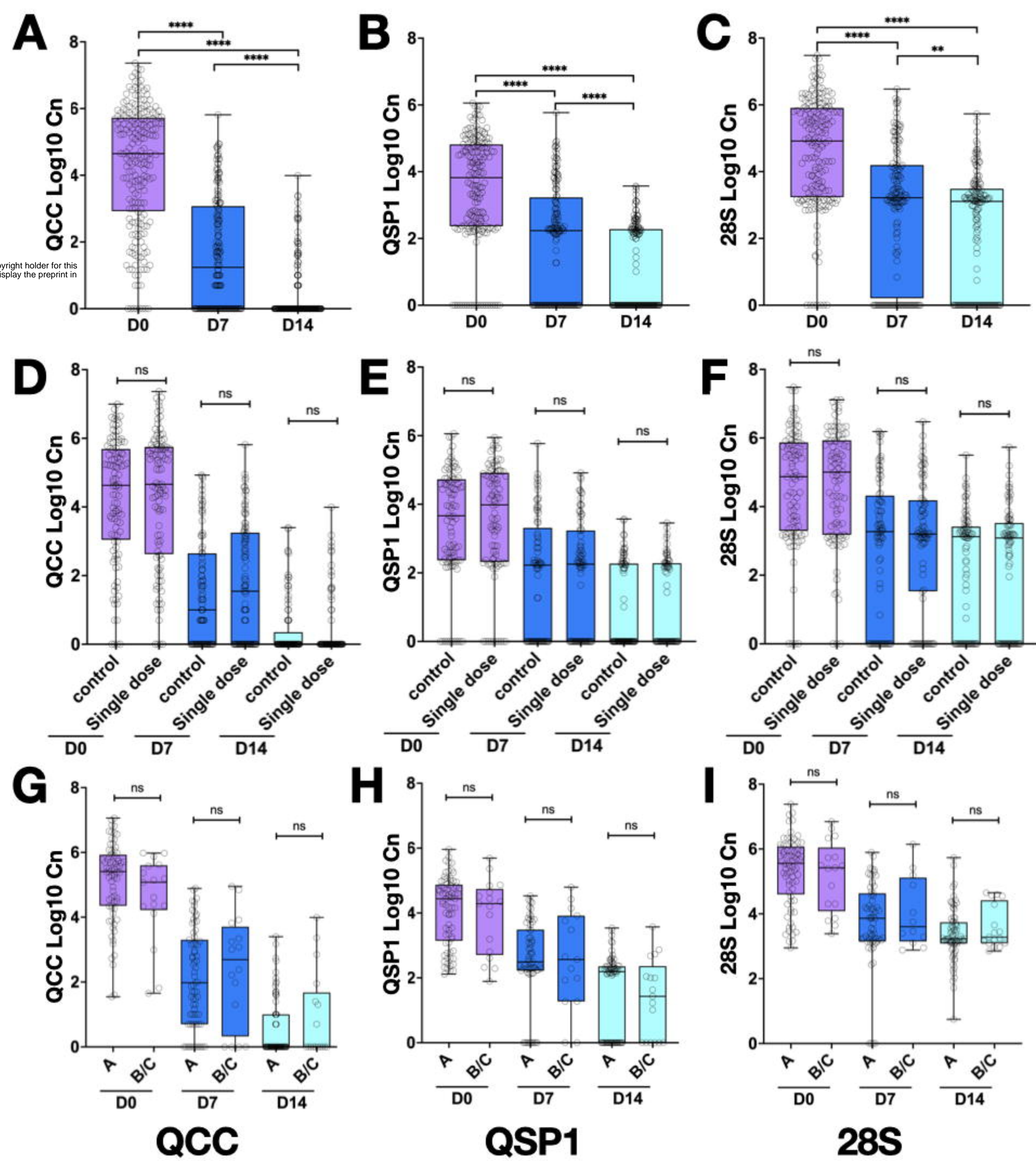


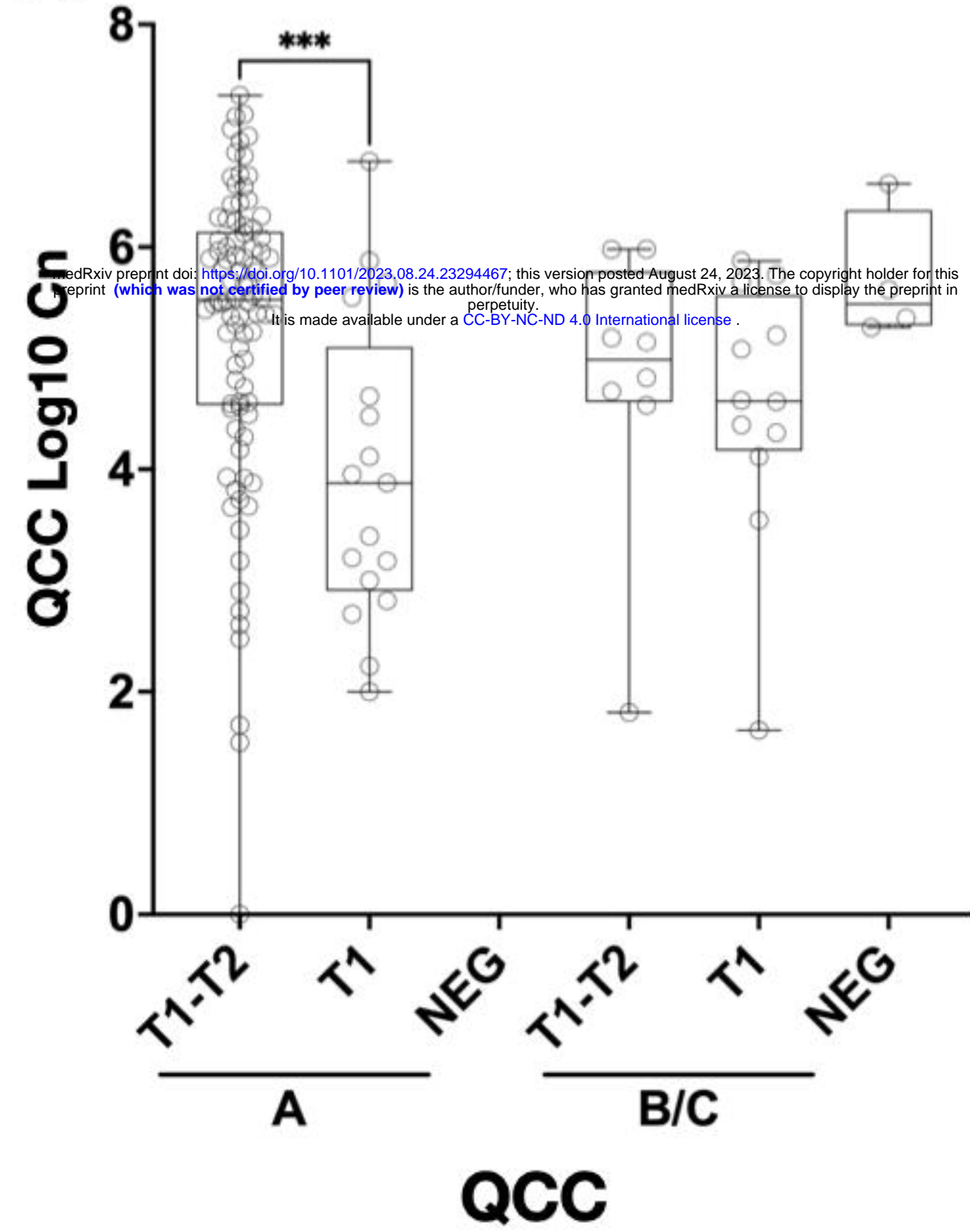
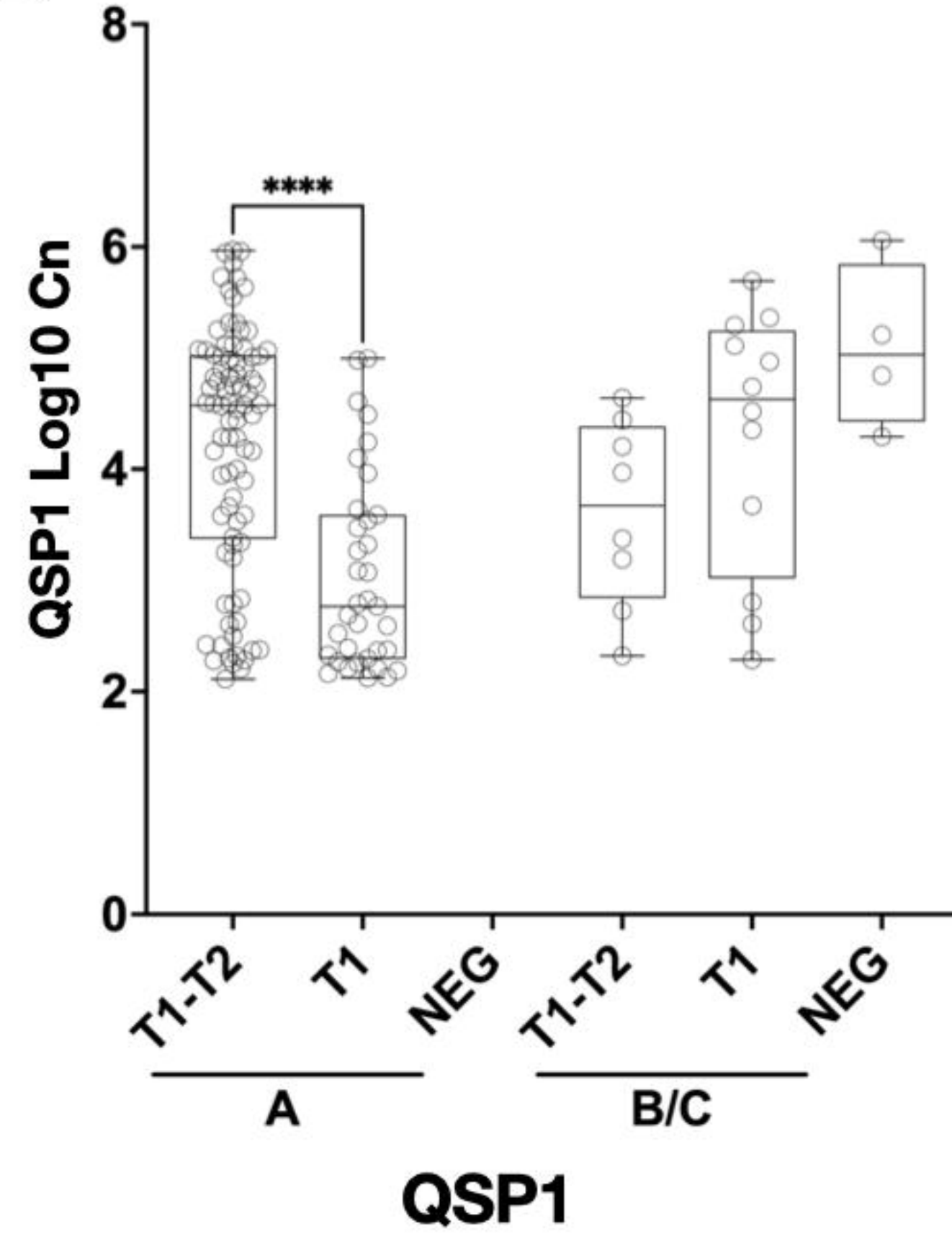
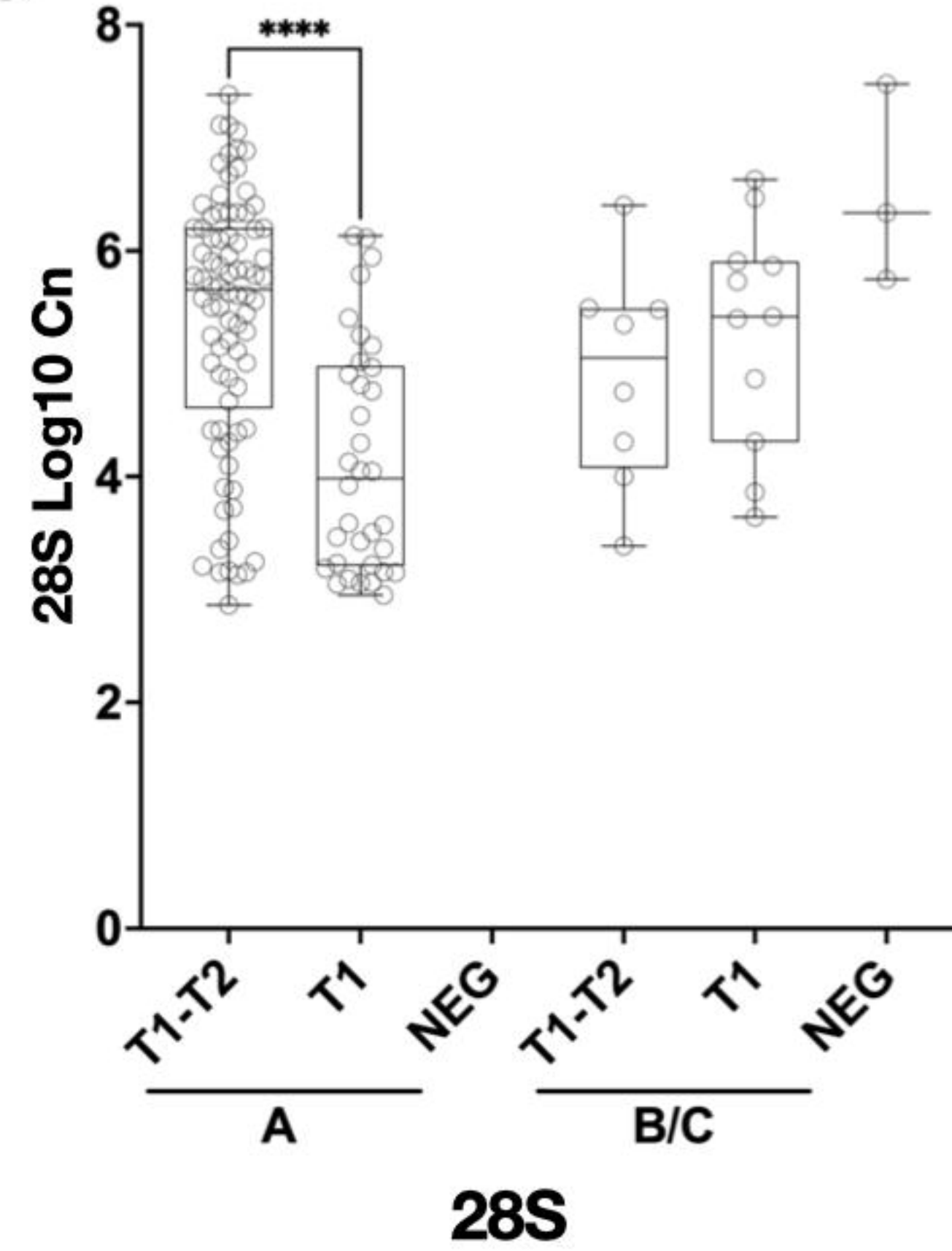
Viability qPCR assay
=> QSP1 RTqPCR

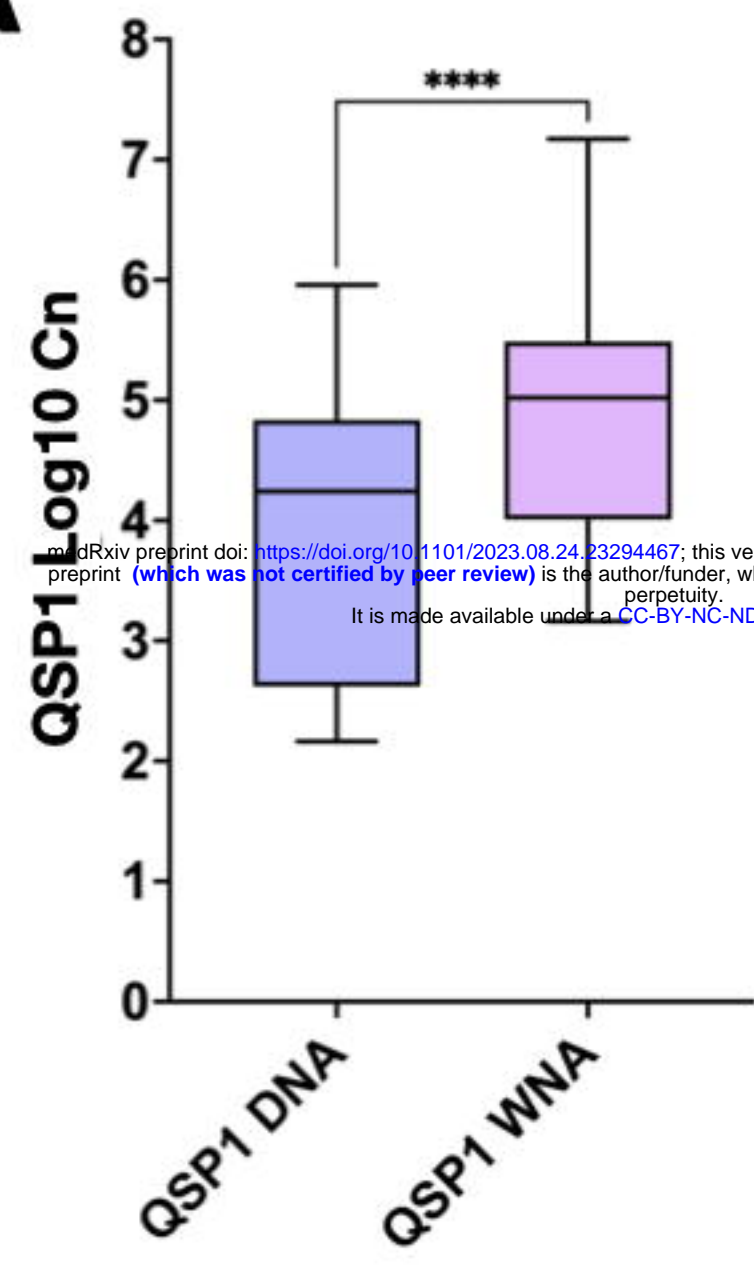
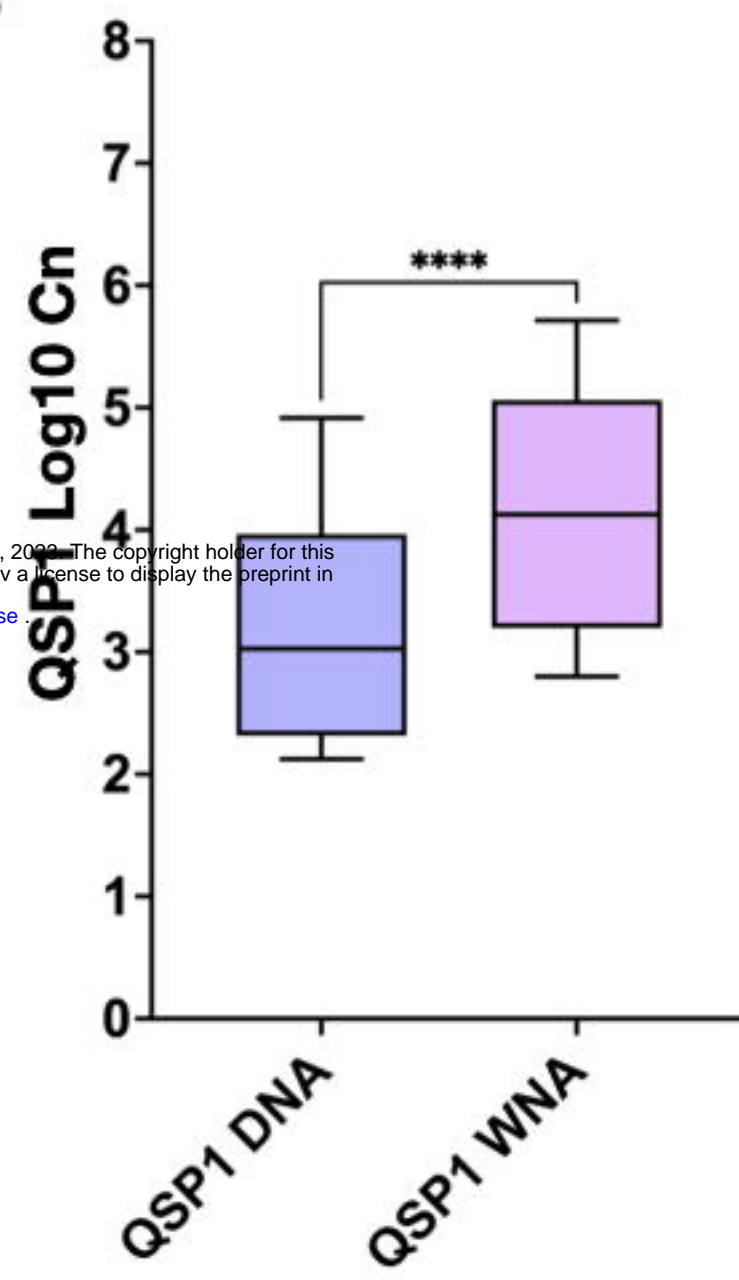
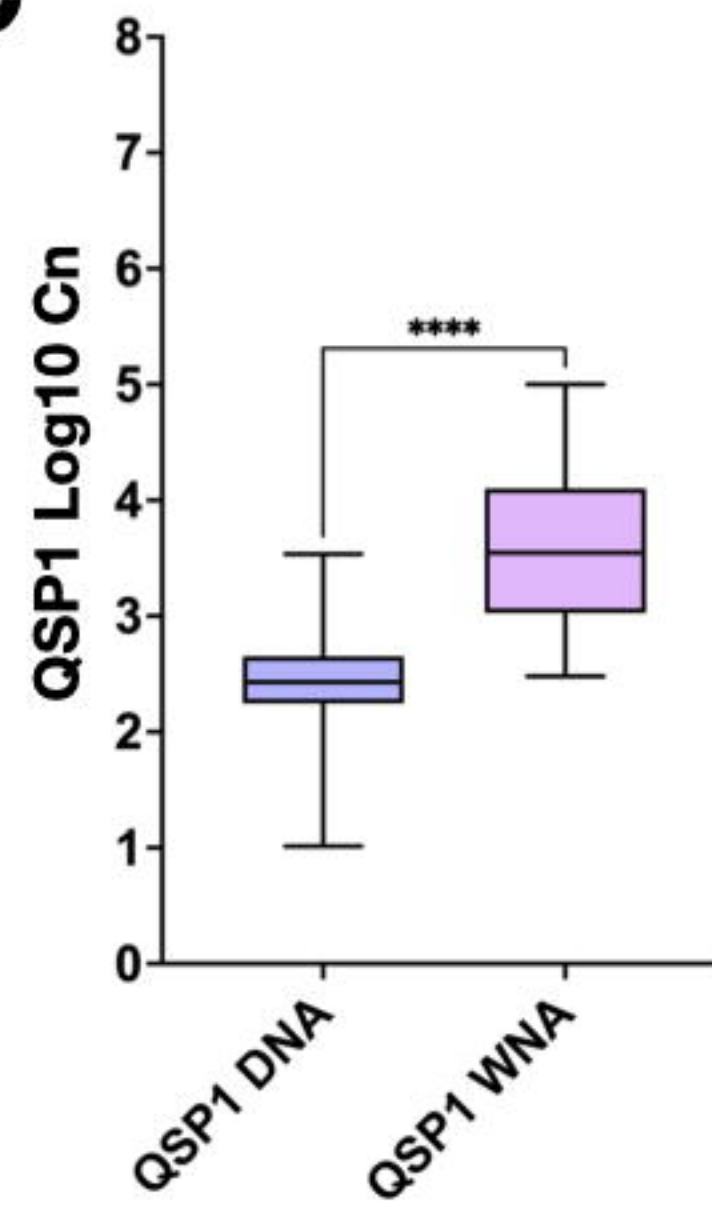
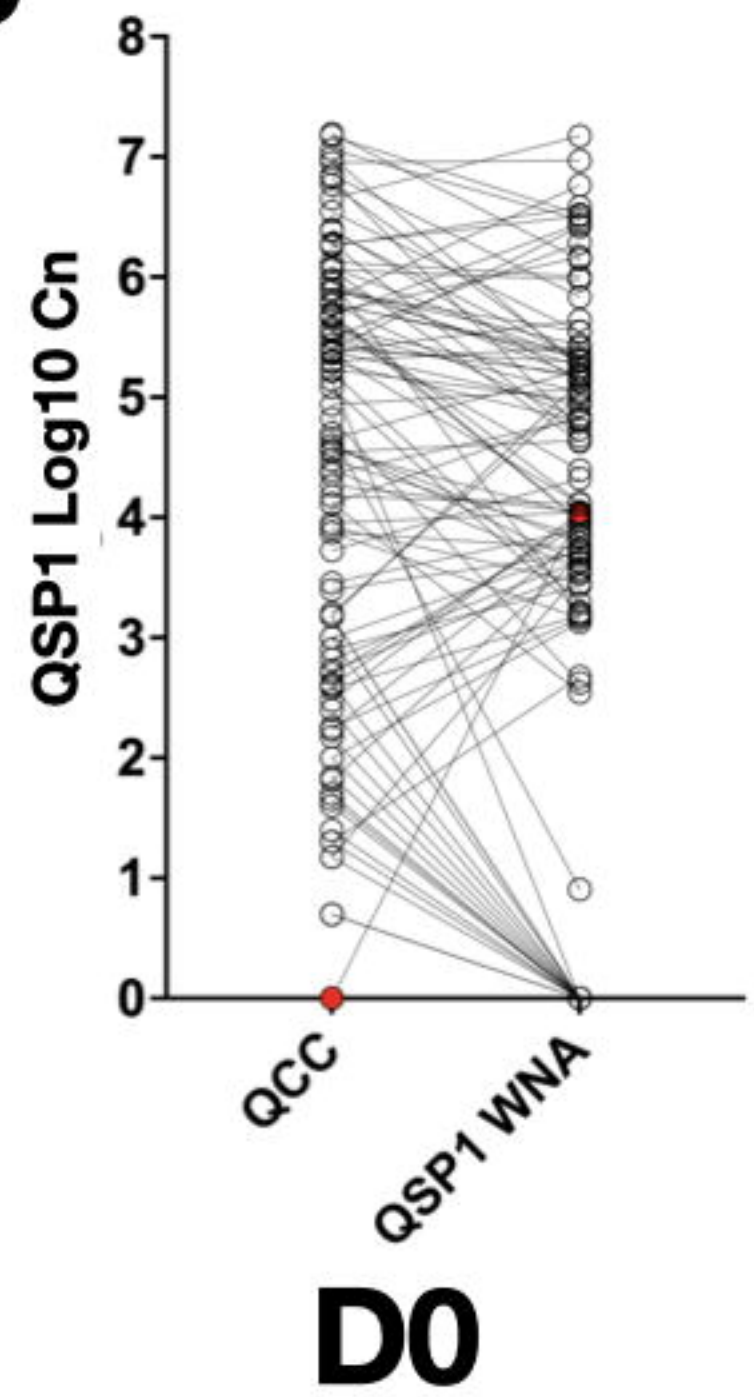
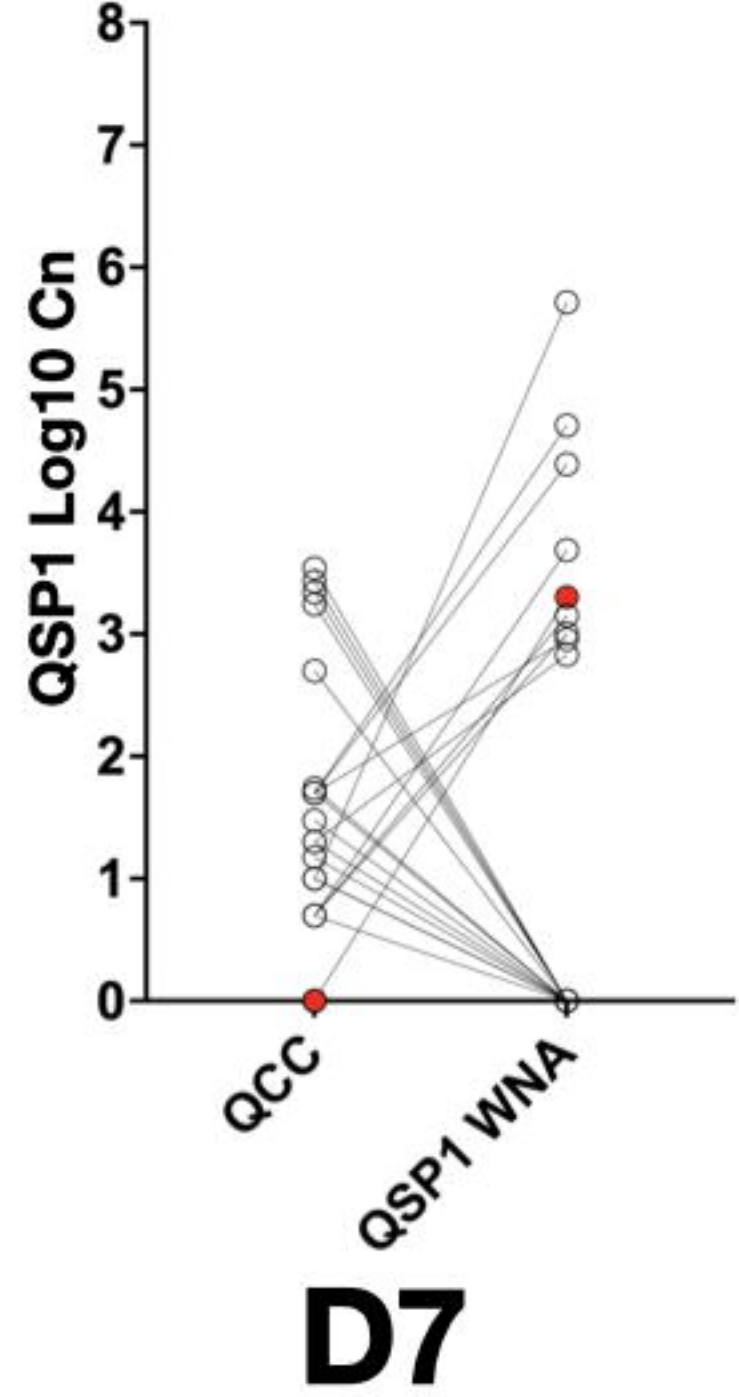
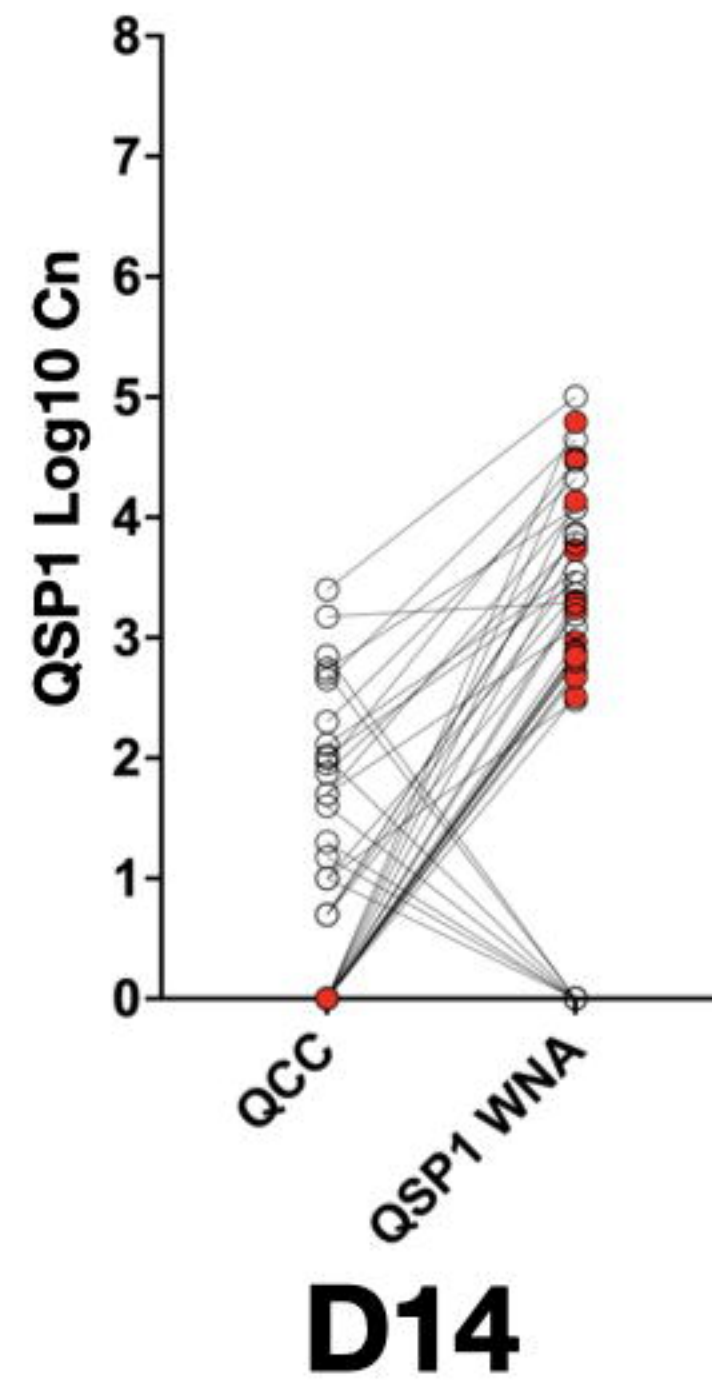


Detection of WNA (RNA+DNA)
in the CSF

A**B****C**



A**B****C**

A**B****C****D****E****F**

medRxiv preprint doi: <https://doi.org/10.1101/2023.08.24.23294467>; this version posted August 24, 2023. The copyright holder for this preprint (which was not certified by peer review) is the author/funder, who has granted medRxiv a license to display the preprint in perpetuity. It is made available under a [CC-BY-NC-ND 4.0 International license](https://creativecommons.org/licenses/by-nc-nd/4.0/).